약학박사학위논문

플라티코딘 D 와 효소에 의해 전환된 플라티코딘 D 강화분획물의 지방축척 억제효과

Effects on lipid accumulation by platycodin D and its enriched fraction produced by cellulase

2019 년 2 월

서울대학교약학대학대학원

천연물과학전공

이은정

ABSTRACT

Effects on lipid accumulation by platycodin D and its enriched fraction produced by cellulase

Eunjeong Lee

Natural Products Science

College of Pharmacy

Doctorate Course in the Graduate School

Seoul National University

Platycodi Radix, the root of *Platycodon grandiflorum* (Jacq.) A. DC. (Campanulaceae), is traditionally used as a treatment for respiratory discomfort by practitioners of Traditional Chinese medicine, Japanese Kampo medicine and Korean medicine. Platycosides, the saponins found in the roots of *Platycodon grandiflorum* (Jacq.) A. DC. (Platycodi Radix), are typically composed of oleanane backbones with two side chains, one is a 3-*O*-glucose side chain linked by a glycosidic bond and the other being a 28-*O*-arabinose-rhamnose-xylose-apiose side chain joined by an ester bond. Platycodi Radix is known to have more than 20 saponins with similar structures. Among them, platycodin D is superior to other saponins and the distinctive compound found only in Platycodi Radix. It is known to be effective for those with a sore throat, bronchitis, cold, diabetes, inflammation and cancer. Although platycodin D has broad pharmacological value, because the total content of saponins is as low as 2% by dry weight of Platycodi Radix, it is difficult to isolate platycodin D from Platycodi Radix on a large scale. When attempting to overcome this disadvantage, we successfully isolated platycodin D in Platycodi Radix and several derivatives in a short period of time using a multi-step process which includes high-speed counter-current chromatography (HSCCC) and preparative reversed-phase high-performance liquid chromatography (HPLC) steps. We also successfully developed an enzyme-conversion technique through which platycodin D_3 (PD_3) and platycoside E (PE),

which have two and three glucose units at C-3, respectively, are converted to platycodin D, consequently increasing the amount of platycodin D in saponin and thus making it an enriched fraction (henceforth PScell).

In this study, we aim to determine the mechanism of how platycodin D, which is widely known to be effective on the bronchus, works on obesity. A second goal is to determine the effects of PScell on obesity.

We initially examined platycodin D and platycodin D derivatives to determine how they inhibit lipid accumulation activity, finding that platycodin D is a more effective inhibitor than any of the platycodin D derivatives. To determine the optimal concentration of platycodin D, various doses were exposed to cells during MDI (isobutylmethylxanthine, dexamethasone and insulin)-induced differentiation. On day 8, the lipid contents in 3T3-L1 cytoplasm were measured by Oil Red O staining. The results showed that platycodin D (1, 2.5, 5 μM) blocked adipocyte differentiation in proportion to the platycodin D dose with platycodin D 5 μM inhibiting lipid accumulation in the cytoplasm by as much as 62.5% in a MDI-treated positive control without affecting cell viability. It was also found that platycodin D significantly inhibits fat accumulation of lipid droplets in the cytoplasm by inhibiting adipogenic-specific transcription factors PPARγ2 and C/EBPα in MDI-induced 3T3-L1 cells in a dose-dependent manner. Similarly, platycodin D inhibits adipocyte differentiation of 3T3-L1 cells through the ERK pathway within 24 hrs. Furthermore, we investigated the molecular mechanism of platycodin D, focusing on its ability to decrease the expression of adipogenic factors through AMP-activated protein kinase α (AMPKα) in adipocytes and to prevent abdominal fat accumulation in high-fat-diet-induced obesity among C57BL/6 mice. To verify the anti-obesity effect *in vivo*, a group of mice ate a normal diet while the others were fed a high-fat diet for eight weeks. The high-fat-diet mice were then divided into three subgroups: termed the aminoimidazole carboxamide ribonucleotide (AICAR) group, the vehicle group and the platycodin D group. It was found that platycodin D significantly reduced fat accumulation by inhibiting adipogenic signal transcriptional factors, in this case peroxisome proliferator-activated receptor γ2 (PPARγ2) and CCAAT/enhancer binding protein α (C/EBPα), through AMPK *in vivo*. Platycodin D also reduced both the body weight and fat mass and consequently improved lipid metabolism by increasing AMPK, as also seen in AICAR group, while also

reducing PPARγ2 and C/EBPα expression levels in adipose tissue. In addition, glutamic oxaloacetic transaminase (GOT) and glutamic pyruvic transaminase (GPT) levels, which are used as indicators of hepatic disease in serum and the size of lipid drops during morphometric observations of fatty liver were significantly reduced in the platycodin D group. Moreover, protein expressions of AMP-activated protein kinase α (AMPKα) increased while sterol regulatory element binding protein-1 (SREBP-1) decreased in the platycodin D group compared to those of the high-fat group (HF). This outcome suggests that platycodin D can be used to inhibit lipid accumulation by reducing the expression levels of adipogenic factors related to the AMPK pathway and that it can be expected to improve lipid metabolism in obesity-associated hepatic lipogenesis.

In addition, we attempted to investigate the fat accumulation effect of PScell, the fraction with an increased platycodin D content, by enzymatic transformation. Treatment of 3T3-L1 adipocytes with PScell (5, 7.5, 10 μg/mL) reduced lipid accumulation in a dose-dependent manner. In a mouse model, oral administration of PScell (70 mg/kg, 6 mL/kg) reduced high-fat-diet-induced body weight gain. Consistently, PScell alleviated total cholesterol, LDL cholesterol, triglyceride and glucose levels in mice serum. Liver and abdominal adipose tissues from the groups treated with PScell exhibited a decreased number of lipid droplets relative to the high-fat control group. PScell showed a stronger inhibitory effect on lipid accumulation at a slightly lower concentration than that of platycodin D numerically in *in vitro and in vivo.*

From these results, we considered that PScell is a potential candidate as a treatment for obesity and fatty liver induced by a high-fat diet by replacing platycodin D with a low yield in Platycodi radix.

Keywords : Lipid accumulation, Platycodi Radix, Platycodin D, 3T3-L1 cell, Obesity, AMPKα

Student Number : 2007-30463

CONTENTS

LIST OF FIGURES

LIST OF TABLE

I. INTRODUCTION

1. Platycodi Radix, platicosides and platycodin D

Platycodi Radix, the root of *Platycodon grandiflorum* (Jacq.) A. DC. (Campanulaceae) has been used in China, Korea, Japan and other Asian countries for more than 2000 years as an ancient and famous herbal drug and food [1]. It has been reported to enhance immune function, bronchitis, asthma, pulmonary tuberculosis, diabetes and inflammatory diseases and so on [2-3]. The constituents found in Platycodi Radix included large amounts of carbohydrate (at least 90%), polysaccharides, platycosides, peptides, polyacetylenic alcohols and fatty acids [4]. Many of the medicinal effects of Platycodi Radix are attributed to the triterpene saponin known as platycosides **(Table 1)** and up to now, more than 30 platycosides have been isolated from Platycodi Radix.

Platycosides are typically composed of an oleanane backbone with two side chains: a glucose unit attached by an ether linkage at the C-3 position of the triterpene and an ester linkage between C-28 and arabinose [5]. Platycodin saponins are responsible for a variety of biological effects, including anti-inflammation, anti-allergy and anti-tumor activities. Platycodin saponins can also augment the immune response and stimulate apoptosis in skin cells [6-9].

Platycodin D (PD) is the major contributor to the biological activity and content of Platycodi Radix [10]. Several previous studies have reported that the bioactivities of PD, the major component of platycosides, are superior to those of other saponins PD consists of an aglycone with one unbranched sugar chain (one monosaccharide residue) attached to C-3, one unbranched sugar chain (four monosaccharide residues) attached to C-28 and no acetyl domain **(Fig. 1)**. This saponin is well known as a potent triterpenoid saponin with various pharmacological activities including to anti-tumor, hyperlipidemia, anti-inflammatory, expectorant agent and anti-nociceptive [11-14].

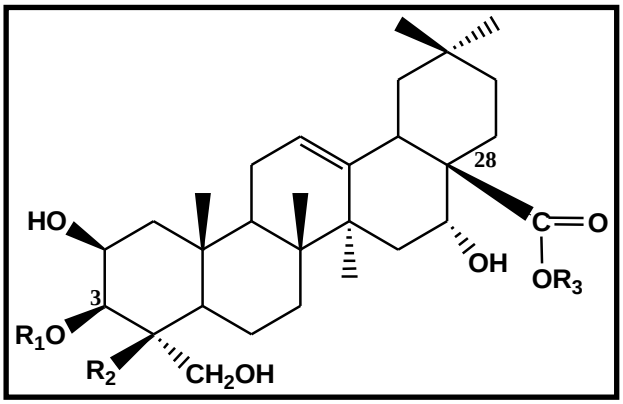

Name	R_1	R_2	R_3
deapio-platycoside E	Glc_6-Glc_6-Glc	CH_2OH	_Ara^2-Rha^4-Xyl
platycoside E	Glc_6-Glc_6-Glc	CH_2OH	_Ara^2-Rha^4-Xyl^3-Api
deapi-platycodin D_3	Glc_6-Glc	CH_2OH	_Ara^2-Rha^4-Xyl
platycodin D_3	Glc_6-Glc	CH_2OH	_Ara^2-Rha^4-Xyl^3-Api
polygalacin D_3	Glc_6-Glc	CH_3	_Ara^2-Rha^4-Xyl^3-Api
deapi-platycodin D	-Glc	CH_2OH	_Ara^2-Rha^4-Xyl
deapi-polygalacin D_3	Glc_6-Glc	CH_3	_Ara^2-Rha^4-Xyl^3-Api
platycodin D	-Glc	CH_2OH	_Ara^2-Rha^4-Xyl^3-Api
platycodin D_2	Glc_3-Glc	CH_2OH	_Ara^2-Rha^4-Xyl^3-Api
polygalacin D	-Glc	CH_3	_Ara^2-Rha^4-Xyl^3-Api
3"-*O*-acetylplatycodin D	-Glc	CH_2OH	_Ara^2-Rha(3-*O*-*Ac*)^4-Xyl^3-Api
polygalacin D_2	Glc_3-Glc	CH_3	_Ara^2-Rha^4-Xyl^3-Api
3"-*O*-acetylplatycodin D_2	Glc_3-Glc	CH_2OH	_Ara^2-Rha(3-*O*-*Ac*)^4-Xyl^3-Api
deapi-polygalacin D_2	Glc_3-Glc	CH_3	_Ara^2-Rha^4-Xyl^3-Api
3"-*O*-acetylplatycodin D_2	Glc_3-Glc	CH_2OH	_Ara^2-Rha(3-*O*-*Ac*)^4-Xyl^3-Api
3"-*O*-acetylplatyconic acid A	-Glc	COOH	_Ara^2-Rha(2-*O*-*Ac*)^4-Xyl^3-Api
2"-*O*-acetylplatycodin D	-Glc	CH_2OH	_Ara^2-Rha(2-*O*-*Ac*)^4-Xyl^3-Api
3"-*O*-acetylplatycodin D_2	Glc_3-Glc	CH_2OH	_Ara^2-Rha(3-*O*-*Ac*)^4-Xyl^3-Api

2"-*O*-acetylplatycodin D_2	Glc_3-Glc	CH_2OH	_Ara^2-Rha(3-*O*-*Ac*)^4-Xyl^3-Api
2"-*O*-acetylplatyconic acid A	-Glc	COOH	_Ara^2-Rha(2-*O*-*Ac*)^4-Xyl^3-Api

Table 1. The structures of various platycosides

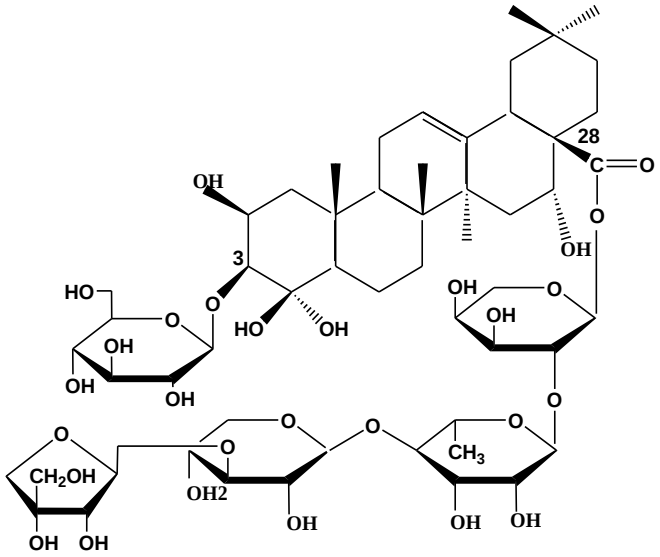

Figure 1. Structure of platycodin D

2. Adipocyte and adipogenesis

Obesity features excessive fat accumulation and storage due to an imbalance between energy intake and energy expenditure [15, 16]. Obesity is a major obstacle to human health, which makes offering to the prevalence of other associated disease such as type 2 diabetes, cancer, hyperlipidemia and cardiovascular disease [17]. Recently, obesity has been medically focused such as metabolic stimulants, appetite suppressant, digestive inhibitor, glucose/insulin metabolism, lipid metabolism and adipocyte specific effect [18]. However, these drug targets used to inhibit fat can cause serious side effects like weight gain, diarrhea, vomiting and increasing glucose in serum [19].

The 3T3-L1 cell line is widely used as an adipocyte differentiation model system for studying the metabolic mechanisms of obesity and the molecular mechanisms of adipogenesis. Obesity is characterized by increased fat mass, which is associated with increased 3T3-L1 preadipocytes cell number (hyperplasia) and mature adipocytes sizes (hypertrophy) **(Fig. 2)** [20, 21]. Adipocyte hypertrophy is caused by excessive accumulation of lipid such as triglyceride (TG) formed from energy intake [22]. Adipocytes hyperplasia results from a complex interaction between proliferation and differentiation in preadipocytes that is involved in the adipogenic process where undifferentiated preadipocytes are converted to differentiated adipocytes [23, 24]. Therefore, adipogenesis and TG accumulation play an important role in fat mass increase. Accordingly, controlling adipogenesis and TG accumulation in adipocytes could help prevent obesity and its associated diseases.

Mature adipocytes constitute the majority of cells in adipose tissue. Besides mature adipocytes, fat tissue contains several other cell types, including stromal-vascular cells (SVC) such as fibroblasts, smooth muscle cells, monocyte, endothelial cells and adipogenic progenitor cells or preadipocytes **(Fig. 3)** [25]. Adipose tissue is divided into two subtypes, white and brown fat. White fat is widely distributed and it represents the primary site of fat metabolism and storage, whereas brown fat is relatively scarce and its main role is to provide body heat, which is essential for newborn babies. White adipose tissue is the major energy reserve and its primary function is to store triacylglycerol (TG) in periods of energy excess and to release

energy in the form of free fatty acids during energy deprivation [26, 27]. Fat tissue also plays an important role innumerous processes through its secretory products and endocrine functions. In the adipose tissue, adipocytes are important cells in maintaining proper energy stability and lipid metabolism by secretion adipokines. Adipokines are a type of bioactive polypeptide and include leptin, adiponectin andtumor necrosis factor-alpha, which are released from adipocytes **(Fig. 4)** [28, 29]. These peptides play a vital role in regulating appetite and energy expenditure and are necessary for modulating insulin along with economic development, the incidence of obesity is increasing insulin sensitivity and fat metabolism.

Adipogenesis is regulated by sequential expression of adipogenic and lipogenic genes. During differentiation, the peroxisome proliferator-activated receptor γ2 (PPARγ2) and CCAAT/enhancer binding protein α (C/EBPα) are two key transcription factors **(Fig. 5)** [30]. PPARγ2, a sub-family of nuclear hormone receptors, activates the gene expression of fatty acid-binding protein and phosphoenol pyruvate carboxykinase to promote lipid synthesis. C/EBPα proteins play a crucial role during the maturation and differentiation of adipocytes. The expression of C/EBPα generates a coordinated effect with PPARγ2 to induce adipogenesis. Subsequently, in the final stage of differentiation, the differentiated cells express markers characteristic of adipocyte phenotype such as ap2 (adipocyte selective fatty acid binding protein), LPL (lipoprotein lipase), ACC (acetyl-CoA carboxylase) and FABP (fatty acid binding protein) [31].

The ERK, p38 and JNK mitogen activated protein kinase (MAPKs) are important to proliferation and differentiation in cellular level **(Fig. 6)** [32]. MAPKs are activated by a large variety of stimuli and one of their major functions is to connect cell surface receptors to transcription factors in the nucleus. MAPK pathways are able to regulate adipogenes is at each steps of the process, from stem cells to adipocytes **(Fig. 7)** [33] and it was reported that inhibition of MAP kinase would block lipogenesis in early stage of 3T3-L1 adipocyte differentiation. While the ERK pathway is involved throughout adipogenesis, displaying both positive and negative effects, p38 and JNK seem to have more restricted potentials which consequently triggers long-term cellular responses.

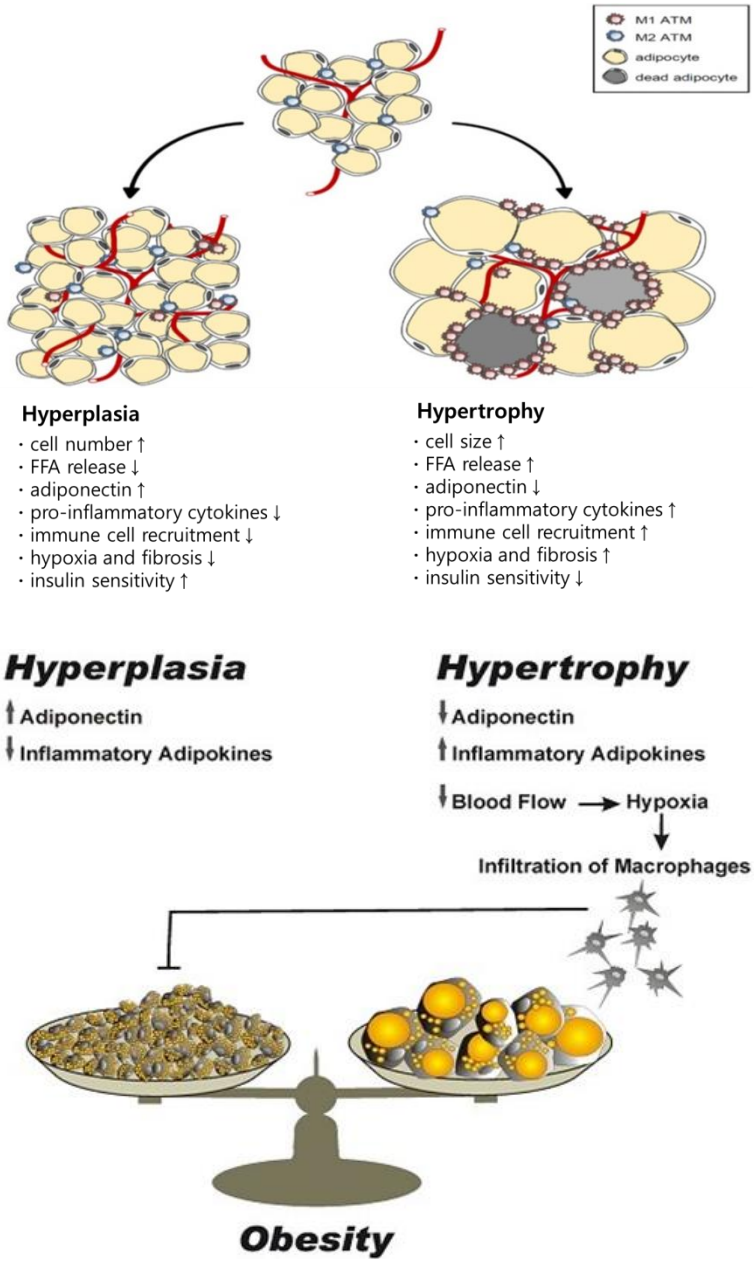

Figure 2. Physiological balance between hypertrophy and hyperplasia (adapted from ref. [71])

Obesity is determined by increasing both the size and number of adipocytes. Adipogenesis can lead to a large number of new adipocytes (hyperplasia) which produce more adiponectin and less inflammatory adipokines. By the other side, hypertrophied adipocytes produce less adiponectin and more inflammatory adipokines. The prevalence of hypertrophied adipocytes in adipose tissue leads to a reduction in blood flow with subsequent hypoxia and macrophage infiltration. In addition, cytokines produced by macrophages inhibit adipogenesis.

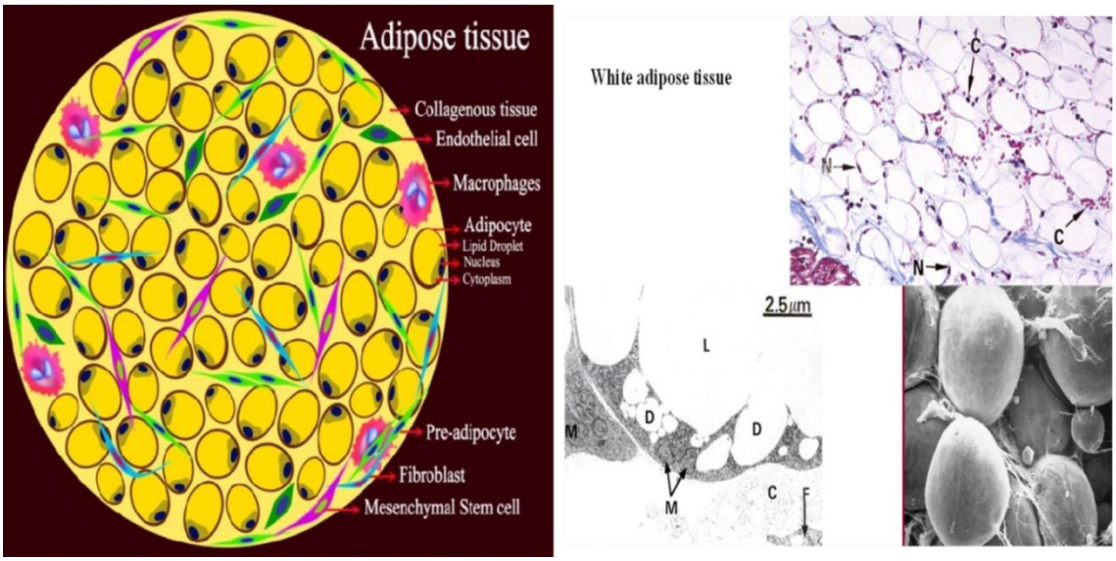

Figure 3. Constitute of cells in white adipose tissue (adapted from ref. [72])

Mature adipocytes constitute the majority of cells in adipose tissue. Besides mature adipocytes, fat tissue contains several other cell types including stromal-vascular cells (SVC) such as fibroblasts, smooth muscle cells, monocyte, endothelial cells and adipogenic progenitor cells or preadipocytes**.**

L: lipid, D: droplet, M: macrophage, C: cytosol

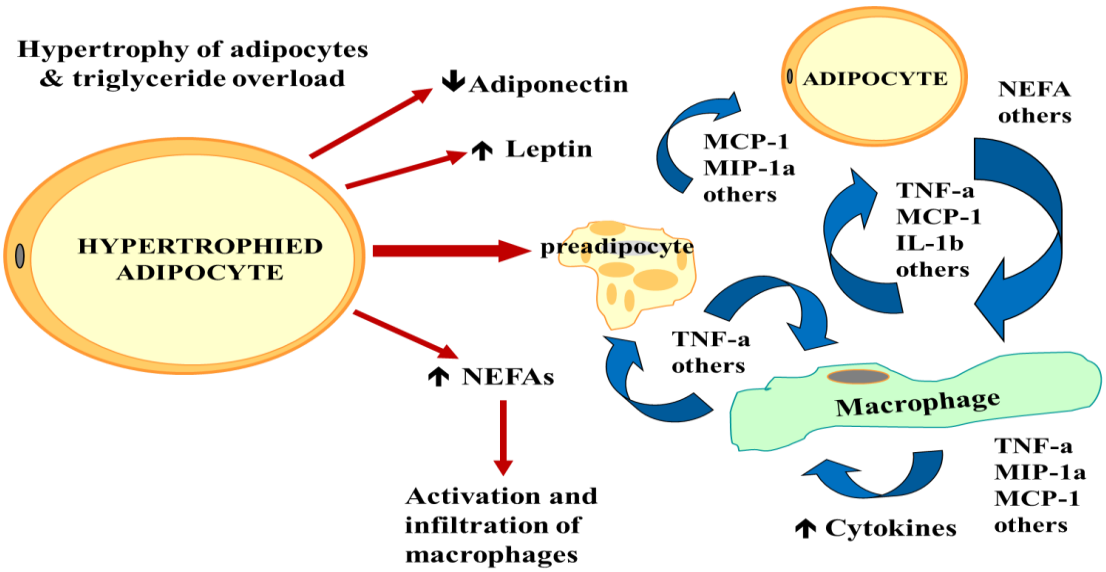

Figure 4. Secretion adipokines of triglyceride overload hypertrophy adipocyte (adapted from ref. [73])

In the adipose tissue, adipocytes are important cells in maintaining proper energy stability and lipid metabolism by secretion adipokines. Adipokines are a type of bioactive polypeptide and include leptin, adiponectin and tumor necrosis factor-alpha, which are released from adipocytes.

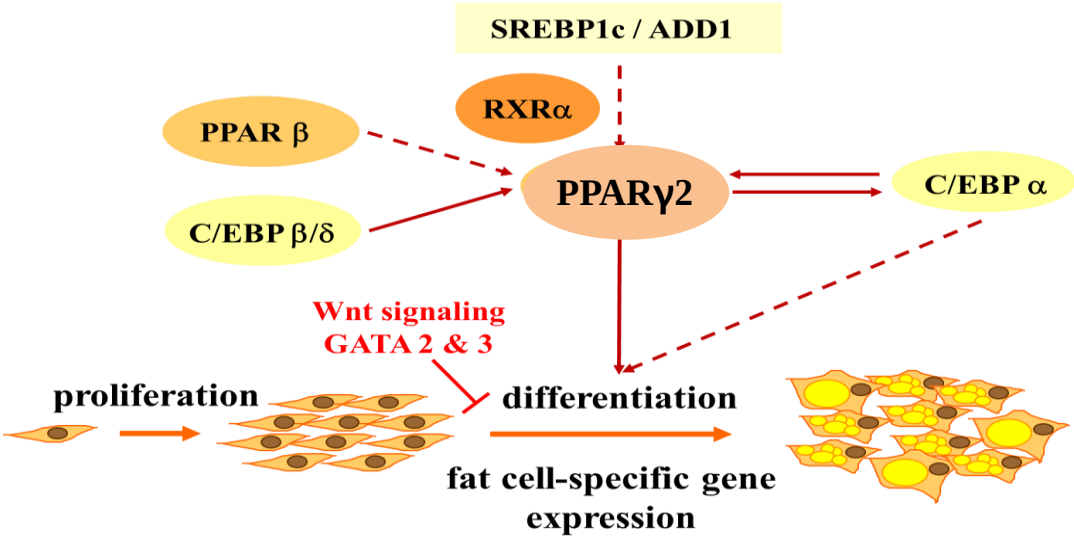

Figure 5. Transcriptional factors of adipocyte differentiation PPARγ2, C/EBPα (adapted from ref. [74])

Adipogenesis is regulated by sequential expression of adipogenic and lipogenic genes. During differentiation, the peroxisome proliferator-activated receptor γ2 (PPARγ2) and CCAAT/ enhancer binding protein α (C/EBPα) are two key transcription factors.

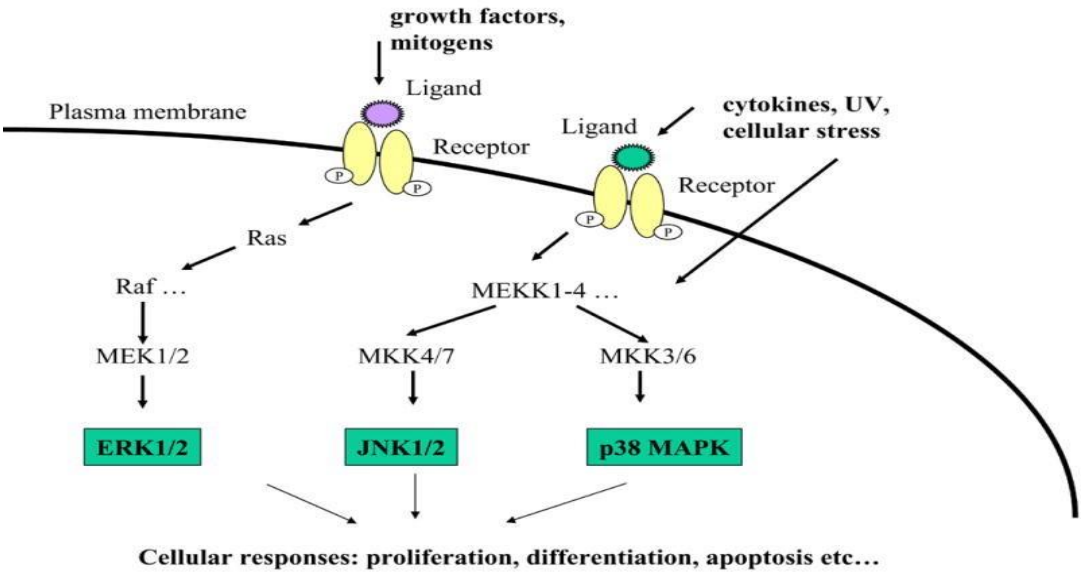

Figure 6. MAPKs signal transduction pathways (adapted from ref. [32])

The ERK, p38 and JNK mitogen activated protein kinase (MAPKs) are important to proliferation and differentiation in cellular level. MAPKs are activated by a large variety of stimuli and one of their major functions is to connect cell surface receptors to transcription factors in the nucleus.

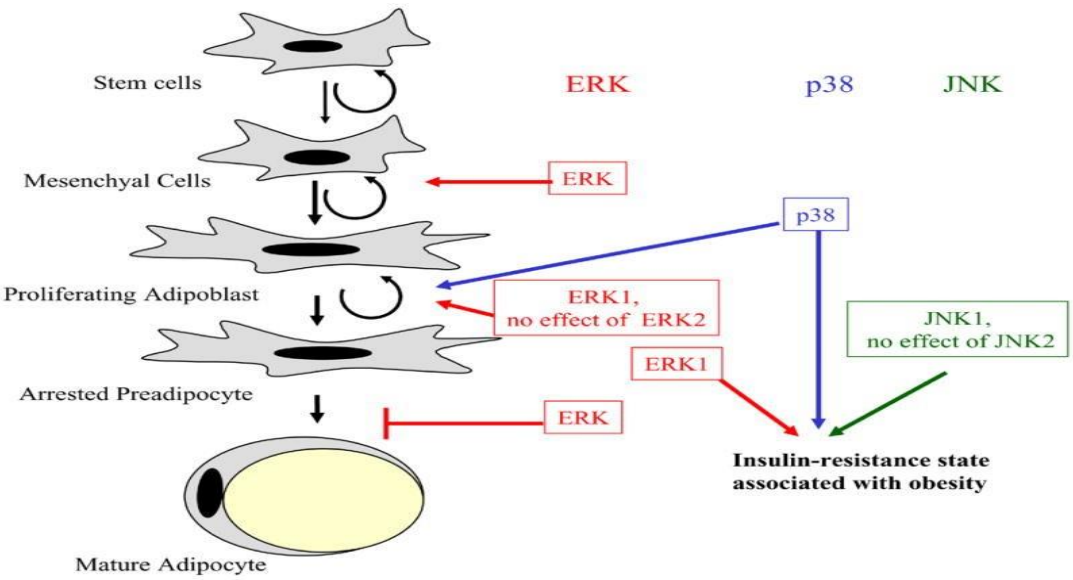

Figure 7. Involvement of the MAPKs at the various steps of adipogenesis (adapted from ref. [32])

MAPK pathways are able to regulate adipogenesis at each steps of the process, from stem cells to adipocytes. MAPK pathways are able to regulate adipogenesis at each steps of the process, from stem cells to adipocytes. It was reported that inhibition of MAP kinase would block lipogenesis in early stage of 3T3-L1 adipocyte differentiation. While the ERK pathway is involved throughout adipogenesis, displaying both positive and negative effects, p38 and JNK seem to have more restricted potentials which consequently triggers long-term cellular responses.

3. AMPK

AMP-activated protein kinase α (AMPKα) is involved in various processes and substances such as oxidation for regulating glucose, lipid metabolism and an enzyme which is likely to be activated in various circumstances with low energy. Once activated, AMPK phosphorylates and inactivates metabolic enzymes associated with ATP-consuming processes such as acetyl CoA carboxylse (ACC) which in turn regulates fatty acid and cholesterol anabolism. Low-level activation of AMPKα has been considered to be involved in the pathogenic development of obesity and diabetes [35].

Adipocytokines, which maintain an anti-inflammatory environment and include IL-10 and adiponectin, are secreted in adipocytes. Activated AMPK promotes production of these adipocytokines. The development of a pro-inflammatory environment within obese adipose tissue is attributed to the excess calorie intake. Adipocytes expand, becoming hypertrophic and often necrotic and subsequently increasing infiltration of macrophages. Production of proinflammatory cytokines and chemokines, as well as macrophage recruitment and M1 polarisation, can be inhibited by activated AMPK, which increases adiponectin secretion and thereby potentially reduces insulin resistance [36].

Fatty acid, which leads to the subsequent increase in the accumulation of total cholesterol and triglyceride, is attributed to high fat diet. Fatty liver is generally ascribed to hepatic lipid accumulation, which is caused by the increased supply of circulating free fatty acids to the liver [37]. The activated AMPK leads to the increased texocytosis of lipoprotein as well as liver fatty acid oxidation. Sterol regulatory element binding protein (SREBP) is a membrane-bound transcription factor which regulates lipid metabolism and is regulated by upstream AMP-activated protein kinase [38]. Chronic activation of AMPK is reported to lead to the decreased SREBP-1 and its target genes, as well as reduce fat storage.

Several agents have been used in the experiments designed for activating AMPK. AICAR (5’-aminoimidazole-4-carboxamide ribonucleoside) is a nucleoside that has been widely used to activate AMPK in intact cells, tissues and animals [39]. AICAR is phosphorylated to the nucleotide ZMP which mimics AMP thereby activating AMPK without

altering adenine nucleotide ratios, once it is transported into cells. Several plant-derived compounds including galegine, berberine and resveratrol, as well as metformin and thiazolidinediones such as rosiglitazone mentioned above, activates AMPK in intact cells by modifying adenine nucleotide ratios [40]. Furthermore, while the lipid-lowering statin drugs, as well as several adipocytokines and hormones such as leptin, adiponectin and ghrelin, have been reported to activate AMPK in certain tissues, the mechanism by which they activate AMPK remains yet to be characterized.

4. Purpose of the study

Platycodin D, a major component isolated from the root of *Platycodon grandiflorum* (Platycodi Radix), is an oleanane triterpene that binds four sugar units at C-28 and a glucose unit at C-3 [5]. Recently, PD has been shown to inhibit lipase and LDL-cholesterol levels [41]. *In vivo*, it has been shown significantly to reduce calorie intake, which increases lipid accumulation [42, 43]. PD also inhibits adipogenesis in 3T3-L1 cells by modulating Kruppel-like factor 2 (KLF-2) and PPARγ2 [44]. However, to the best of our knowledge, there is little evidence correlating the effects of PD on lipid accumulation in adipocytes and adipose tissue.

Therefore, this study aimed to characterize the effects of a PD treatment on lipogenesis *in vitro* and to elucidate the underlying *in vivo* mechanisms in high-fat-diet-induced obese mice. PD was separated from Platycodi Radix using column chromatography and preparative high-performance liquid chromatography (Prep-HPLC) [45, 46]. However, conventional separation methods are tedious, time-consuming and require multiple steps, which can result in the irreversible adsorptive loss of the sample in the stationary phase and can often entail artifact formation. Due to the low content of PD in Platycodi Radix, conventional methods are not suitable for the separation of PD. High-speed counter current chromatography (HSCCC), an all-liquid partition chromatography, eliminates the irreversible adsorptive loss of the sample onto a solid support matrix column and has excellent sample recovery compared to conventional methods [47]. Our lab successfully developed an efficient method for the isolation and purification of PD via a one-step separation step using preparative HSCCC.

Enzymatic transformation has been widely used to modify natural and/or synthesize organic compounds [48]. It provides excellent benefits, such as stereo specificity and mild reaction levels as well as a low cost and simple control of the reaction. Our lab utilized the most powerful enzyme to convert the compounds and optimized the conditions to obtain higher amounts of PD based on a HSCCC-HPLC analysis. We successfully developed an enzyme-conversion technique through which PD_3 and PE, which have two and three glucose units at C-3, respectively, are converted to PD, consequently increasing the amount of PD in saponin and thus making it an enriched fraction (PScell).

Another purpose of this study is to confirm the effects on fat accumulation by this fraction (PScell) now that it has been separated efficiently is available commercially.

Ⅱ. MATERIALS and METHODS

1. MATERIALS

1.1. Plant material

Platycodi Radix was purchased at a local herbal market in Seoul. It was identified by Dr. Je Hyun Lee, Dong Kuk University. A voucher specimen (SNUNPRI-1015) was deposited at the Herbarium of the Natural Products Research Institute in Seoul National University.

1.2. Chemicals and reagents

All organic solvents used for extraction and column chromatography purchased from Duksan Chemical Co., in Korea.

1.3. Cell culture

3T3-L1 preadipocytes were purchased from American Type Culture Collection. Dulbecco's modified Eagle's medium (DMEM), Dulbecco's phosphate-buffered saline (D-PBS), penicillin, streptomycin, trypsin-EDTA, trypan blue, 3-isobutyl-1-methylxanthine (IBMX), dexamethasone (DEX), Oil Red O, LEPAL CA-630 (NP-40), recombinant human insulin, 4-(2-hydroxyethyl)-1-piperazineethane-sulfonic acid (HEPES), naphthylethylenediamine dihydrochloride and AICAR (98% purity) were purchased from Sigma Aldrich. Dimethylsulfoxide (DMSO) was purchased from Bioshop. Bovine calf serum (BCS) was obtained from Abclone. Fetal bovine serum (FBS) was purchased from South Pacific. The cell counting kit-8 was purchased from Dojindo laboratories. Polyvinylidene difluoride (PVDF) membrane was purchased from Millipore and protein assay reagent was obtained from Bio-Rad. PPARγ2 (goat polyclonal IgG, SC-22022), C/EBPα (goat polyclonal IgG, SC-61), p-AMPKα (Thr 172, rabbit polyclonal IgG, SC-33524), AMPKα (goat polyclonal IgG, SC-22022), p-ACC (Ser-79, rabbit polyclonal IgG, SC-111) and ACC (goat polyclonal IgG, SC-22022) were obtained from Santa Cruz Biotechnology. ECL plus detection kit was purchased from Amersham.

1.4. Animals

C57BL/6 mice (male, 5-weeks old) were supplied from Samtako (Osan, Korea). The animals were fed with a standard laboratory diet water *ad libitum* (12 hr light/dark cycle; temperature 22 ± 2℃). The animal study was approved by the Animal Ethics Committee of Seoul National University, the guidelines of which are in accordance with the Guide for the Care and Use of Laboratory Animals as adopted and promulgated by the National Institutes of Health.

1.5. Apparatus

The HPLC analysis was carried out on a Hitachi L-6200 instrument equipped with UV detector system (ELSD) and a SIL-9A auto injector (Shimadzu, Japan). Separation were carried out a Zorbax SB-Aq C_{18} column (150 mm × 4.6 mm, 5 μM particle size, Agilent Technologies, Palo Alto, CA, USA). A-TBE-300A HSCCC (Shanghai Tauto Biotech Co. Ltd., Shanghai, China) with three serially connected multilayer coil separation column (Tubing I. D.= 1.6 mm, total volume = 260 mL, sample loop = 20 mL) was operated at a speed of revolution that ranged from 0 to 1000 rpm. A different TBE-20A HSCCC (Shanghai Tauto Biotech Co. Ltd., Shanghai, China) with three multilayer coil separation column (Tubing I. D.= 0.8 mm, total volume = 16 mL, sample loop = 200 ul) was operated at a speed of revolution that ranged from 0 to 1800 rpm.

2. METHODS

2.1. Preparation of crude sample

The dried Platycodi Radix was extracted by sonication with water for 3 hr at room temperature. The extraction procedure was repeated three times. The extracts were combined and evaporated to dryness under reduced pressure. The crude extract was loaded onto a reversed-phase C_{18} open column (50 × 3 cm i.d.; the volume of the column was 250 mL) and sequentially eluted with water, and 30 and 70% methanol. The enriched platycosides fraction was eluted with 70% methanol from the crude extract of Platycodi Radix. This fraction was evaporated, lyophilized and stored in a refrigerator for the subsequent HSCCC separation.

2.2. One-step separation of platycodin D by HSCCC

HSCCC was performed with a two-phase solvent system composed of ethyl acetate/n-butanol/water (1.2:1:2, v/v) for the separation of platycodin D (PD). The multilayer-coiled column was filled with the upper phase (stationary phase) and the lower phase (mobile phase) simultaneously using the HPLC pump according to a 70:30 volume ratio. Only the lower phase was pumped at a flow rate of 1 mL/min and the apparatus was rotated at 850 rpm. The eluent was collected in glass tubes with a fraction collector and peak fractions were combined based on a similar elution profile determined by HPLC-ELSD.

PD was separated and characterized as described in the previous report PD was preparatively purified from the platycodi radix by high speed counter current chromatography (HSCCC) [10]. The purity of PD was over 95% by HPLC analysis and its structure is shown in **Fig. 8**.

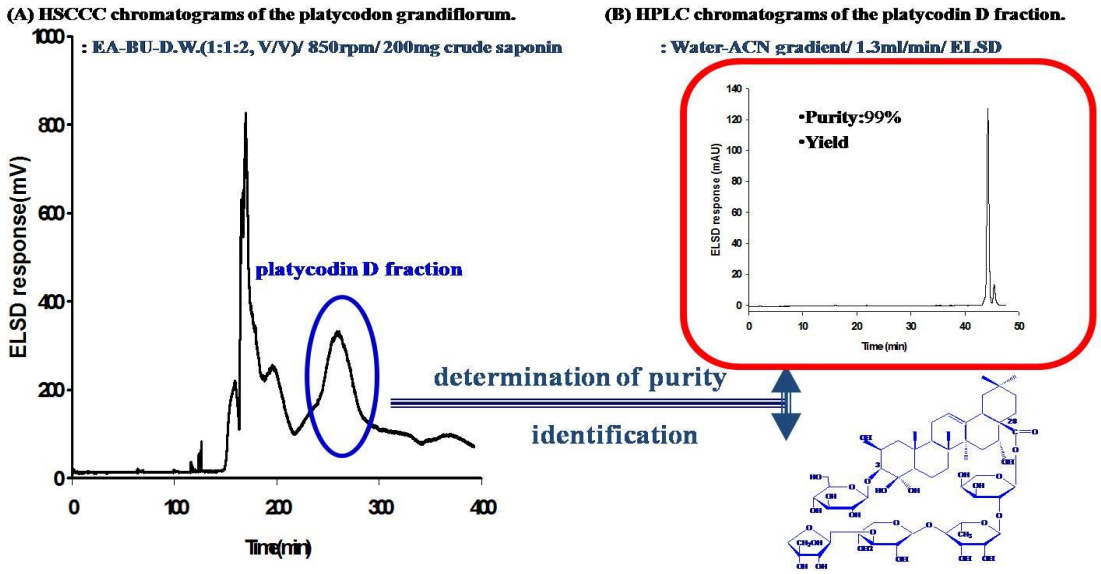

Figure 8. Sampling-preparative isolation platycodin D from *Platycodon grandiflorum* A. DC. by HSCCC coupled with ELSD

HSCCC was performed with a two-phase solvent system composed of ethyl acetate/n-butanol/water (1.2:1:2, v/v) for the separation of platycodin D (PD). The eluent was collected in glass tubes with a fraction collector and peak fractions were combined based on a similar elution profile determined by HPLC-ELSD. The purity of PD was over 95% by HPLC analysis.

2.3. Large-scale modification of the saponin-enriched fraction for platycodin D (PScell)

PScell is an enzyme conversion technique sample through which PD_3 and PE, which have two and three glucose units at C-3 respectively, are converted to PD, consequently increasing PD amounts in saponin and thus making it enriched fraction **(Fig. 9)**.

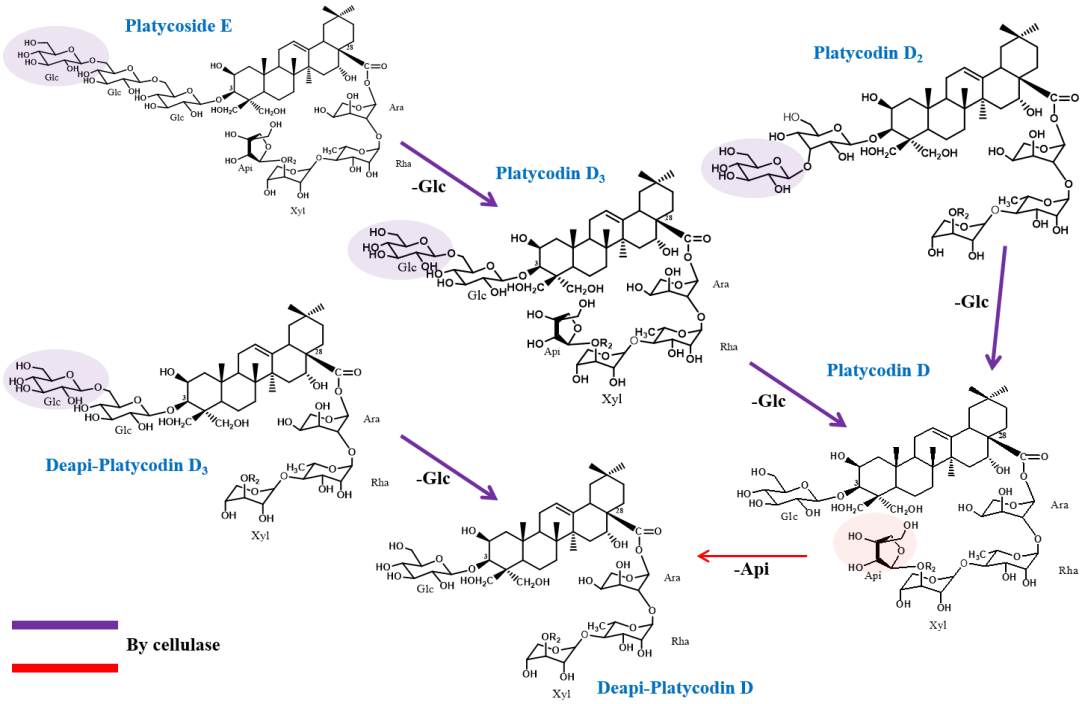

Figure 9. Enzymetic biotransformation of the saponin-enriched fraction to platycodin D by cellulase

PScell is an enzyme conversion technique sample through which PD_3 and PE, which have two and three glucose units at C-3 respectively, are converted to PD, consequently increasing PD amounts in saponin and thus making it enriched fraction.

The reaction mixture containing platycosides (PS) (1 and 2 g) and cellulase (200 and 400 units) in pH5 buffer was incubated at 37.5℃ for 24 hr in a shaking incubator and placed in a water bath at 90℃ to stop the reaction. The reacted mixture was loaded onto a Diaion-HP 20 open column and sequentially eluted with water, 30% methanol and 100% methanol. The 100% methanol fractions (PScell enzymatically transported product) was evaporated, lyophilized and stored in a desiccators until HPLC-ELSD and ESI/MS analysis (**Fig. 10)**.

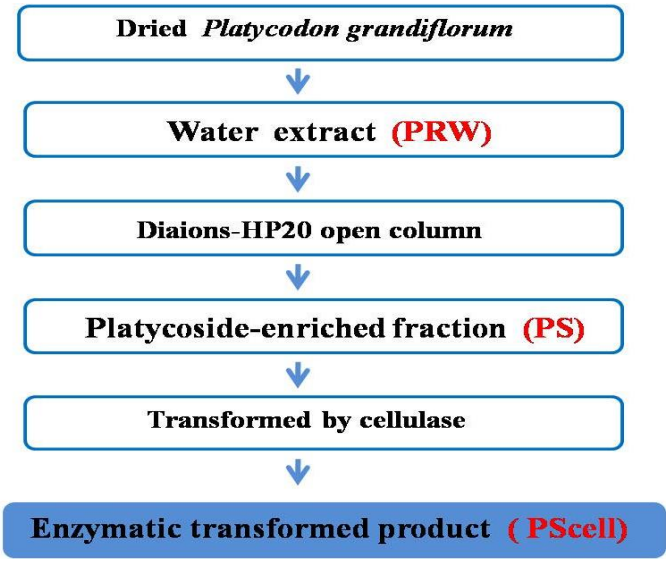

Figure 10. Large-scale modification of the saponin-enriched fraction for platycodin D

The reaction mixture containing platycosides (PS) (1 and 2 g) and cellulase (200 and 400 units) in pH5 buffer was incubated at 37.5℃ for 24 hr in a shaking incubator and placed in a water bath at 90℃ to stop the reaction. The reacted mixture was loaded onto a Diaion-HP 20 open column and sequentially eluted with water, 30% methanol and 100% methanol. The 100% methanol ftactions (PScell enzymatically transported product) was evaporated, lyophilized and stored in a desiccators until HPLC-ELSD and ESI/MS analysis.

2.4. Cell viability assay.

Cell cytotoxicity was evaluated by MTT assay [49]. 3T3-L1 preadipocyte cells were seeded at a density of 5×10^4 per well in 96-well plates and stabilized at 37℃ for 24 hr. The cells were treated with various concentrations of sample for 48 hr in triplicate. The MTT solution (5 mg/ml) was added to each well, and the cells were incubated for another 4 hr at 37℃ in 5% CO_2 incubator. The formazan crystals were dissolved by addition of 200 µl of DMSO. After 30 min, the amount of colored formazan derivative was determined by measuring optical density (OD) using the ELISA microplate reader (Emax, Molecular Devices, CA, USA) at 595 nm.

2.5. Adipocyte differentiation and treatment

3T3-L1 mouse embryo fibroblasts were grown in DMEM with 10% BCS containing 25 mM HEPES, 25 mM $NaHCO_3$, 100 units/mL of penicillin, and 100 µg/mL of streptomycin (growth medium) at 37℃ in 5% CO_2. Cells were seeded at a density of 5×10^4 cells/well in a 6-well plate containing 2 mL of growth medium in each well. The cells were then incubated for two days until they became confluent. At this stage, differentiation was induced by exchanging the media with the fresh ones including mediated differentiation inducer (MDI), 10% FBS, 0.5 mM IBMX, 1 µM DEX and 10 µg/mL insulin for two days (from day 0 to day 2). After two days, the media was replaced with DMEM containing 10% FBS and 10 µg/mL insulin, and the cells were incubated for an additional two days (from day 2 to day 6). This media was changed every other day **(Fig. 11)**.

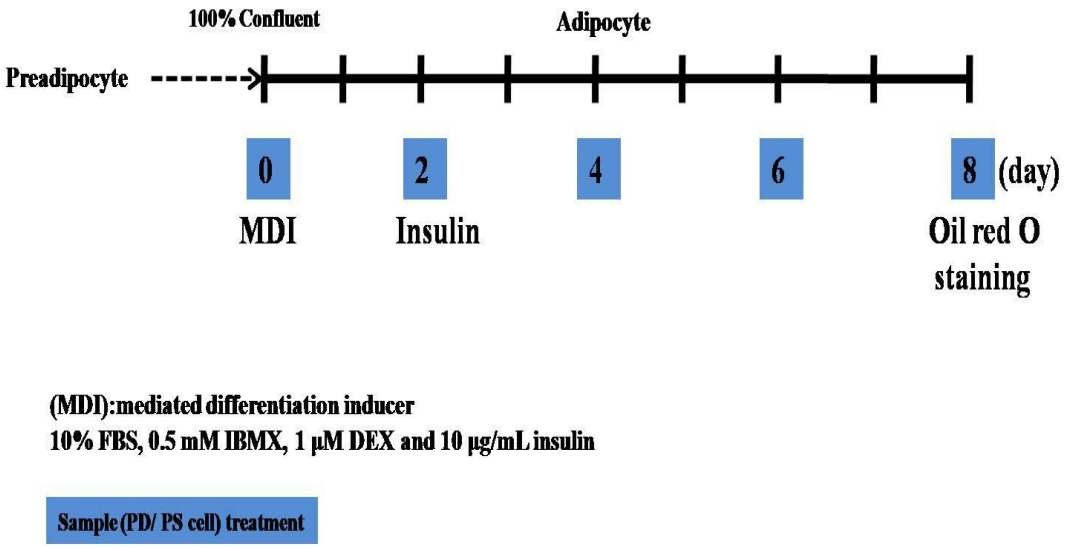

Figure 11. Adipocyte differentiation and treatment

Adipocyte differentiation was induced by exchanging the media with the fresh ones including mediated differentiation inducer (MDI), 10% FBS, 0.5 mM IBMX, 1 µM DEX and 10 µg/mL insulin for two days (from day 0 to day 2). After two days, the media was replaced with DMEM containing 10% FBS and 10 µg/mL insulin and the cells were incubated for an additional two days (from day 2 to day 6). Adipocytes were stained with Oil Red O on day 8 after the induction of differentiation.

2.6. Oil Red O staining

Adipocytes were stained with Oil Red O on day 8 after the induction of differentiation. The cells were washed twice with PBS and fixed with 10% formaldehyde for 1 hr. The cells were then washed twice with distilled water followed by staining with 0.5% Oil Red O solution (in 60% isopropyl alcohol) for 2 hr at room temperature. Cells were washed three times with 60% isopropanol to remove unbound dye and were observed under a Leicafluorescence microscope at magnification × 400. Stained Oil Red O was eluted with 4% NP-40 in isopropanol (v/v) and was quantified by measuring the absorbance at 490 nm.

2.7. Western blot analysis

3T3-L1 cells were extracted in ice-cold lysis buffer containing 20 mM Tris-Cl pH 7.5, 150 mM NaCl, 1 mM Na_2EDTA, 1 mM EGTA, 1% NP40, 1% sodium deoxycholate, 2.5 mM sodium pyrophosphate, 1 mM Na_3VO_4, 1 mM dithiothreitol (DTT), 1 mM phenylmethanesulfonyl fluoride (PMSF) and a protein inhibitor cocktail for 1 hr. Proteins (25 μg/lane) were loaded onto a 12.5% sodium dodecyl sulphate polyacrylamide gel (SDS-PAGE) and then transferred to a nitrocellulose membrane. The membrane was blocked with 5% skim milk in Tris-buffered saline (TBS-T, 50 mM Tris-HCl, pH 7.6 NaCl, 0.05% Tween 20). Then it was incubated with primary antibodies (PPARγ2, C/EBPα, p-AMPKα, AMPKα, p-ACC, ACC) for 3 hr and washed three times in TBS-T. The membrane was incubated with secondary antibodies conjugated with horseradish peroxidase (HRP). Proteins were visualized using a chemiluminescent substrate kit from AB frontier.

For the Western blot of *in vivo* samples, each tissue of the groups were pulverized on dry ice and then homogenized in ice-cold lysis buffer (25 mmol/L HEPES, pH 8.0, 5 mmol/L EDTA, 1% sodium deoxycholate, 1% Triton X-100, 0.1% SDS and protease inhibitors). Homogenized tissues (25% w/v) were centrifuged at 10,000 × g for 20 min at 4℃. The homogenized mixture was then centrifuged, and the supernatant was collected. After discarding the pellet, the protein concentration in the supernatant was determined by the Lowry method [50]. The membranes were scanned with a Bio Rad GS-670 densitometer and the band intensity

was semi-quantified with the UN-SCAN-IT gel & graph digitizing software for Windows (Silk Scientific Inc., USA). The density was measured at five points for each band. Data were presented as the mean density of sample bands relative to that the control bands (β-actin, ACC and AMPK) in the same sample. The experiments were repeated three times.

2.8. RNA isolation and reverse-transcription-polymerase chain reaction (RT-PCR)

Total RNA was isolated using Trizol reagent according to the manufacturer's instructions. Total RNA (2 μg) was converted to cDNA using an RT premix kit from Bioneer according to the instructions. The cDNA population was amplified using a PCR premix kit and compared with the concurrently measured glyceraldehyde-3-phosphate dehydrogenase (GAPDH) expression level. The sequence of primers corresponding to mouse adipogenic genes is as follows: FAS (forward, 5'-CAG TAT AAG CCC AAG GCC AA-3'; reverse, 5'-TAG CCC TCC CGT ACA CTC AC-3'); aP2 (forward, 5'-AAA TCA CCG CAG ACG ACA G-3'; reverse, 5'-AAA TTT CCA TCC AGG CCT CT-3'); GAPDH (forward, 5'-AGA ACA TCA TCC CTG CAT CC-3'; reverse, 5'-TCC ACC ACC CTG TTG CTG TA-3').

2.9. High fat diet animal model experiments

2.9.1. PD treatment

One group of C57BL/6 was fed a normal diet (Samyangsa) and others were fed with a high-fat diet containing casein 26%, maltodextrin 16%, sucrose 9%, lard 32%, soybean oil 3% and mineral mix 1% with a calorie content of 5.4 kcal/g (D-12492, Research diets) for 8 weeks (n=7). The high fat diet mice were then assigned to one of three subgroups. Group 1: The vehicle was orally administered to mice; Group 2: AICAR was *i.p.* injected to mice (64.5 mg/kg body weight, dissolved in PBS, injection volume 0.5 mL); Group 3: PD was orally administered (15 mg/kg body weight, dissolved in PBS, injection volume 0.5 mL). Food intake and body weight were recorded every 3 days for 8 weeks. The mice were sacrificed after 8 weeks for tissue and serum analysis **(Fig. 12A)**.

2.9.2. PScell treatment

In the same manner as in the above test method, one group of C57BL/6 was fed a normal diet (Samyangsa). The high fat diet mice were then assigned to one of four subgroups. Group 1: The vehicle was orally administered to mice; Group 2: PRW (250 mg/kg body weight, dissolved in PBS, injection volume 6 mL/kg); Group 3: PScell (30 mg/kg body weight, dissolved in PBS, injection volume 6 mL/kg); Group 4: PScell (70 mg/kg body weight, dissolved in PBS, injection volume 6 mL/kg). Food intake were recorded once a week and body weight twice a week. The mice were sacrificed after 8 weeks for tissue and serum analysis **(Fig. 12B)**.

A.

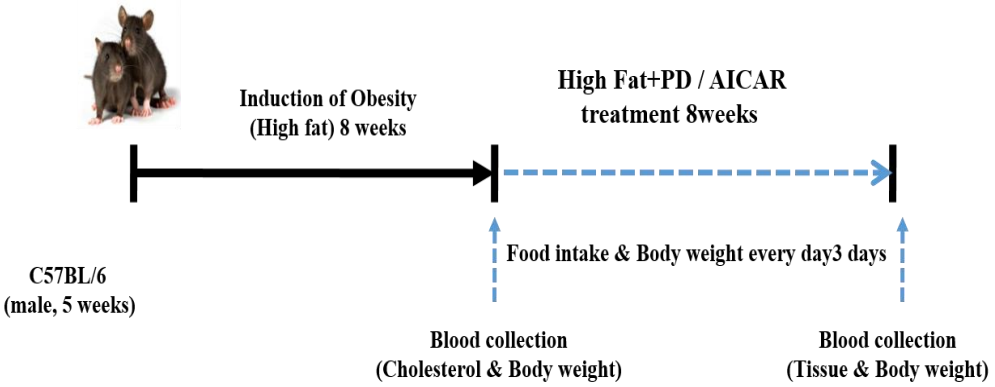

Group 1: Normal diet
Group 2: High fat diet
Group 3: AICAR *i.p.* (64.5 mg/kg body weight, injection volume 0.5 mL)
Group 4: PD oral (15 mg/kg body weight, injection volume 0.5 mL)

B.

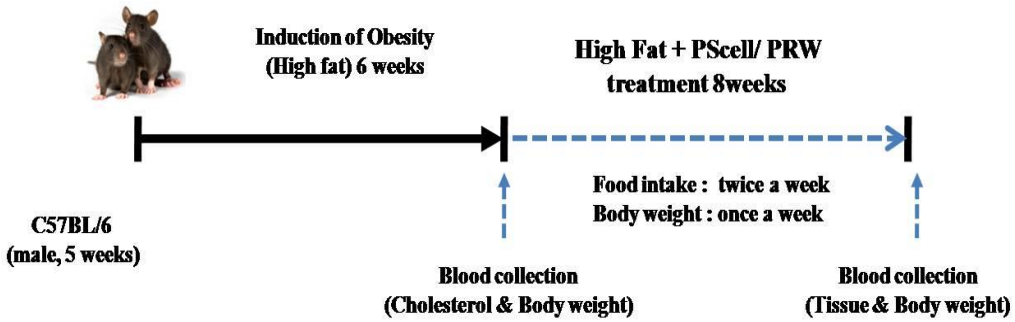

Group 1: Normal diet
Group 2: High fat diet
Group 3: PRW (250 mg/kg body weight)
Group 4: PScell (30 mg/kg body weight)
Group 5: PScell (70 mg/kg body weight)

Volume: 6 mL/kg

Figure 12. High fat diet animal model experiments

A. PD treatment

One group of C57BL/6 was fed a normal diet (Samyangsa) and others were fed with a high-fat diet containing casein 26%, maltodextrin 16%, sucrose 9%, lard 32%, soybean oil 3% and mineral mix 1% with a calorie content of 5.4 kcal/g (D-12492, Research diets) for 8 weeks (n=7). The high fat diet mice were then assigned to one of three subgroups. Group 1: The

vehicle was orally administered to mice; Group 2: AICAR was *i.p.* injected to mice (64.5 mg/kg body weight, dissolved in PBS, injection volume 0.5 mL); Group 3: PD was orally administered (15 mg/kg body weight, dissolved in PBS, injection volume 0.5 mL). Food intake and body weight were recorded every 3 days for 8 weeks. The mice were sacrificed after 8 weeks for tissue and serum analysis.

B. PScell treatment

In the same manner as in the above test method, one group of C57BL/6 was fed a normal diet (Samyangsa). The high fat diet mice were then assigned to one of four subgroups. Group 1: The vehicle was orally administered to mice; Group 2: PRW (250 mg/kg body weight, dissolved in PBS, injection volume 6 mL/kg); Group 3: PScell (30 mg/kg body weight, dissolved in PBS, injection volume 6 mL/kg); Group 4: PScell (70 mg/kg body weight, dissolved in PBS, injection volume 6 mL/kg). Food intake were recorded once a week and body weight twice a week.

2.10. Serum analysis

All mice were fasted for 15 hr prior to being sacrificed. Blood samples were taken from the orbit and centrifuged for the determination of biochemical parameters. The serum was stored at -70℃ until used for assays. High density lipoprotein cholesterol (HDL-C), low density lipoprotein cholesterol (LDL-C), plasma triglyceride (TG), total cholesterol (TC), glutamic oxaloacetic transaminase (GOT) and glutamic pyruvic transaminase (GPT) were assayed using a commercial kit (Asan Pharmaceutical Inc.). The leptin assay kit was obtained from Bio-Rad.

2.11. Micro-computed tomography

Scanning was done using a cone-beam type in vivo micro-CT scanner (Skyscan model 1076, Skyscan, Kontich, Belgium). All animals were scanned under anesthesia (injection of ketamine/xylaxine, 100 mg/mL). The acquisition settings were as follows: x-ray source voltage 50 kVp, current 200 A, a 1 mm thick aluminum filter was used for beam hardening reduction. The pixel size was 35 μm; exposure time was 4.7 seconds, and the rotation step was 0.6° with a complete rotation over 360°.

2.12. Hematoxylin and eosin staining

The adipose tissues of mice and liver were immediately fixed in 10% formalin solution for 24 hr. These tissues were subsequently dehydrated with a series of ethanol solution, from 75% to 100%, before being embedded in paraffin wax. Cross sections were cut at 4 μm and were stained with hematoxylin and eosin. The sections were imaged by light microscopy (Olympus). The sectional areas of white adipose tissue (WAT) were analyzed for the purpose of quantifying the size of adipocytes.

2.13. Statistics

Data are reported as means ± SD. To analyze the data statistically, we performed one-way analysis of variance (ANOVA) for repeated measurements of the same variable and used Duncan's multiple range *t*-test using a SPSS software (version 14) to determine which means were significantly different from that of the control. We considered differences significant at $p< 0.05$.

III. RESULTS

3.1. Cytotoxicity and Lipid accumulation inhibition activities of PD and PD derivatives isolated by HSCCC

We initially examined PD and PD derivatives to determine how they inhibit lipid accumulation activity, finding that PD is a more effective inhibitor than any of the PD derivatives. To determine the cytotoxicity of platycosides isolated by HSCCC, 3T3-L1 cells were treated with various concentrations (0.625-250 μM) of platycosides for 48 hr. Cell viability was evaluated by MTT assay and the results are expressed as a percentage of vehicle control (curve line). 3T3-L1 cells were differentiated with MDI complex in the absence or presence of 9 series (5 μM) for eight. Lipid droplets accumulated in cells were stained with Oil Red O on day 8 after the induction of differentiation and the results expressed as a percentage of vehicle control (graph). As a shown in **Fig. 13**, PD has more cytotoxicity and is more effective on lipid cell inhibition in relatively less concentration. Thus, we implemented the screening process on lipid accumulation in 3T3-L1 cell, targeting PD.

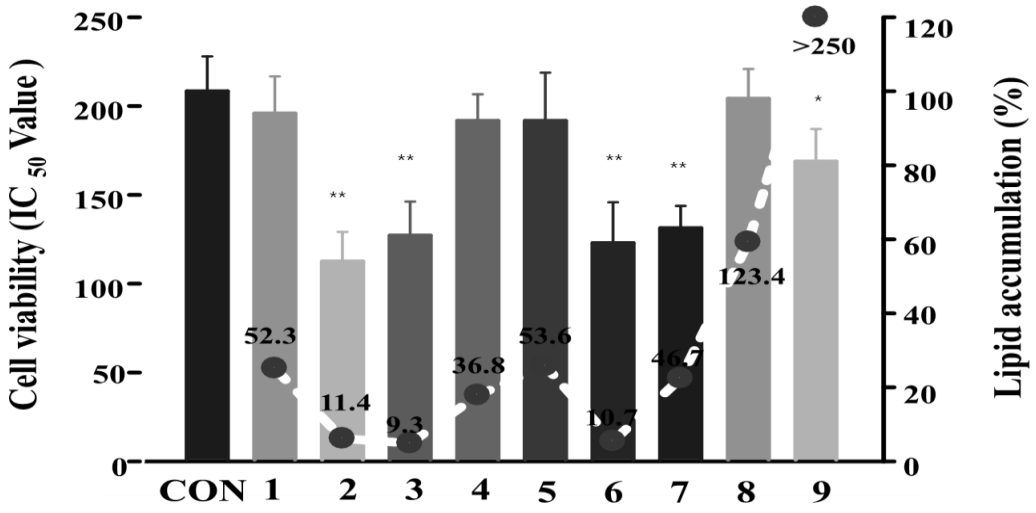

Figure 13. Cytotoxicity and lipid accumulation inhibition activities of platycodin D and platycodin D derivatives

3T3-L1 cells were treated with various concentrations (0.625-250 μM) of platycosides for 48 hr. Cell viability was evaluated by MTT assay and the results are expressed as a percentage of vehicle control (curve line). 3T3-L1 cells were differentiated with MDI complex in the absence or presence of 9 serise (5 μM) for eight. Lipid droplets accumulated in cells were stained with Oil Red O on day 8 after the induction of differentiation and the results expressed as a percentage of vehicle control (graph).

1) deapi-platycodin D, 2) Platycodin D, 3) Polygalacin D, 4) 3"-O-acetyl platycodin D, 5) 3"-O-acetyl polygalacin D, 6) 2"-O-acetyl platycodin D, 7) 2"-O-acetyl polygalacin D, 8) PD-deC3 (de-C3-platycodin D), 9) PD-de28 (de-C28-platycodin D).

3.2. Effects of PD on lipid accumulation during adipocyte differentiation

To find the optimal concentration of PD, cells were treated with various doses of PD (1, 2.5, 5 μM) during MDI-induced differentiation. After inducer treatment, we investigated the effect of PD on lipid accumulation in preadipocytes. While the PD concentration was maintained for 7 days, dose-dependent inhibition of lipid accumulation was observed in the cytoplasm **(Fig. 14A)**. 5 μM PD effectively reduced the lipid content to 62.4% of positive control in differentiated 3T3-L1 adipocytes **(Fig. 14B)**. PPARγ2 and C/EBPα, a master regulator of adipogenesis, were significantly increased with the progression of adipocyte differentiation. PD treatment at 2.5 to 5 μM significantly blocked the expression of these key adipogenic transcription factors **(Fig. 14C)**. Furthermore, treatment with 5 μM PD reduced the expression of FAS and aP2 mRNA levels, well-known downstream factors of PPARγ2 and C/EBPα, as compared to untreated differentiating cells **(Fig. 14D)**.

A.

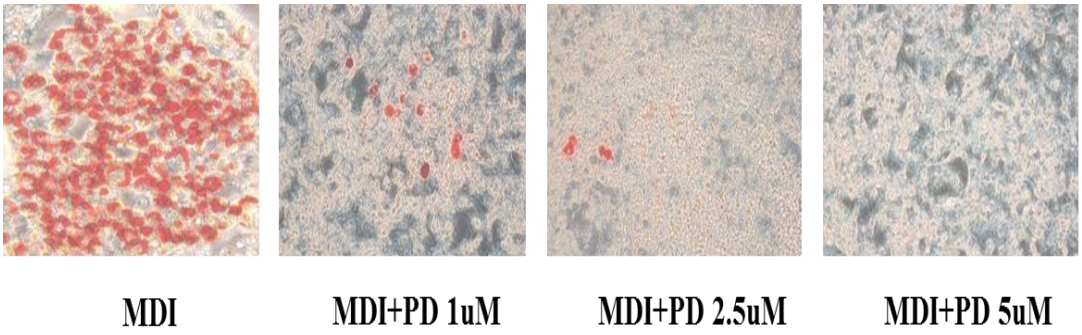

B.

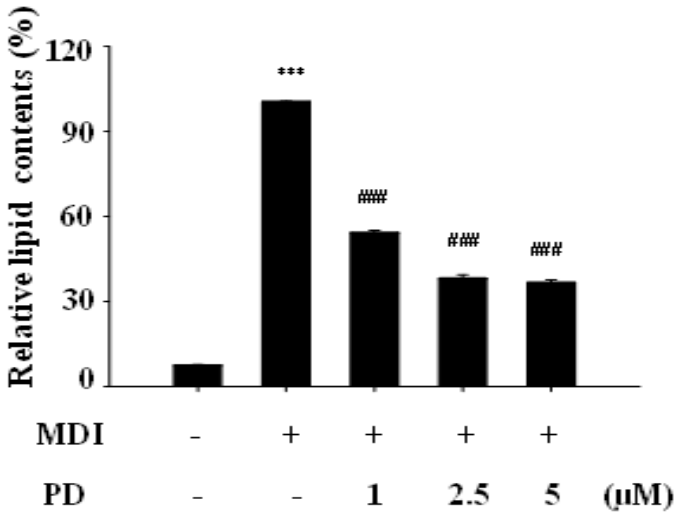

Figure 14. Effects of platycodin D on lipid accumulation during adipocyte differentiation.

(A) Cells were stained with Oil Red O on day 8 after the induction of differentiation. (B) Stained Oil Red O was eluted with 4% NP-40 in isopropanol (v/v) and the absorbance was measured at 490 nm with a spectrophotometer. The error bars represent the standard deviations of means. Different superscripts indicate significant difference at $p<0.05$ according to Duncan's multiple comparison; n=3, ** $p<0.05$, *** $p<0.001$ compared to the differentiated control.

C.

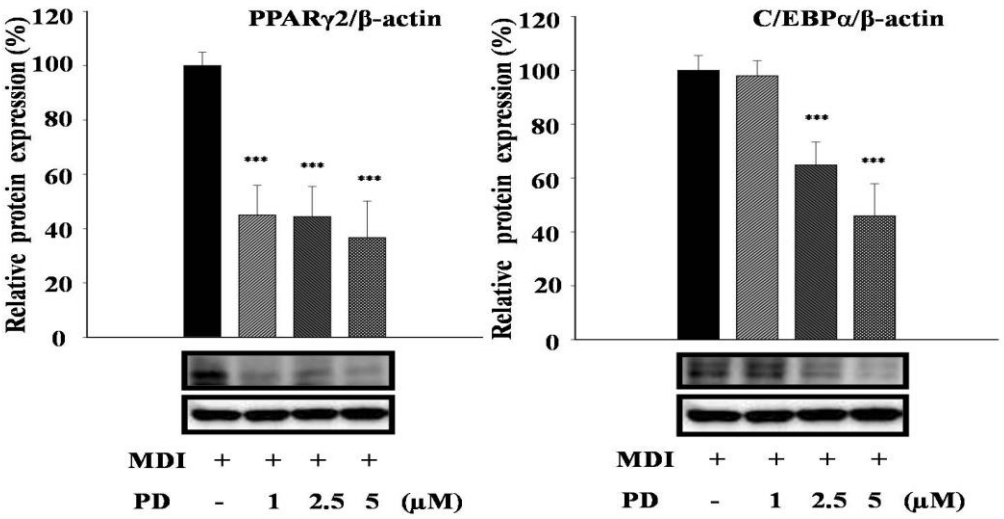

D.

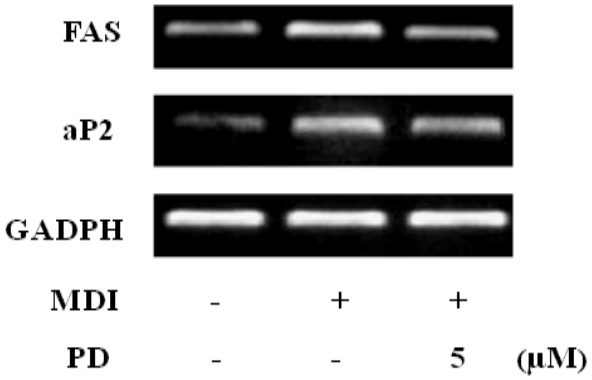

Figure 14. Effects of platycodin D on lipid accumulation during adipocyte differentiation.

(C) PPARγ2 and C/EBPα expression on day 5 were analyzed by Western blot and quantitated. (D) On day 7, mRNA levels of FAS and aP2, which are downstream of PPARγ2 and C/EBPα were detected by reverse-transcription-polymerase chain reaction. The error bars represent the standard deviations of means. Different superscripts indicate significant difference at $p<0.05$ according to Duncan's multiple comparison; n=3, ** $p<0.05$, *** $p<0.001$ compared to the differentiated control.

3.3. Effects of PD on the expression of p-ERK during adipocyte differentiation

Some studies have been reported that MAPK pathway regulates proliferation and differentiation of 3T3-L1 cell [32]. Therefore, to investigate the affection of MAPK pathway in the action of PD 5 μM, adipocyte-induced MDI were harvested designed time during 24 hr. The result shown that p-ERK was increased steadily within 6 hrs whereas PD treatment significantly inhibited the p-ERK activation from 3 hrs to 24hrs. The result suggested the inhibition of adipocyte differentiation by PD was associated with ERK pathway during early stage of adipocyte differentiation **(Fig. 15)**.

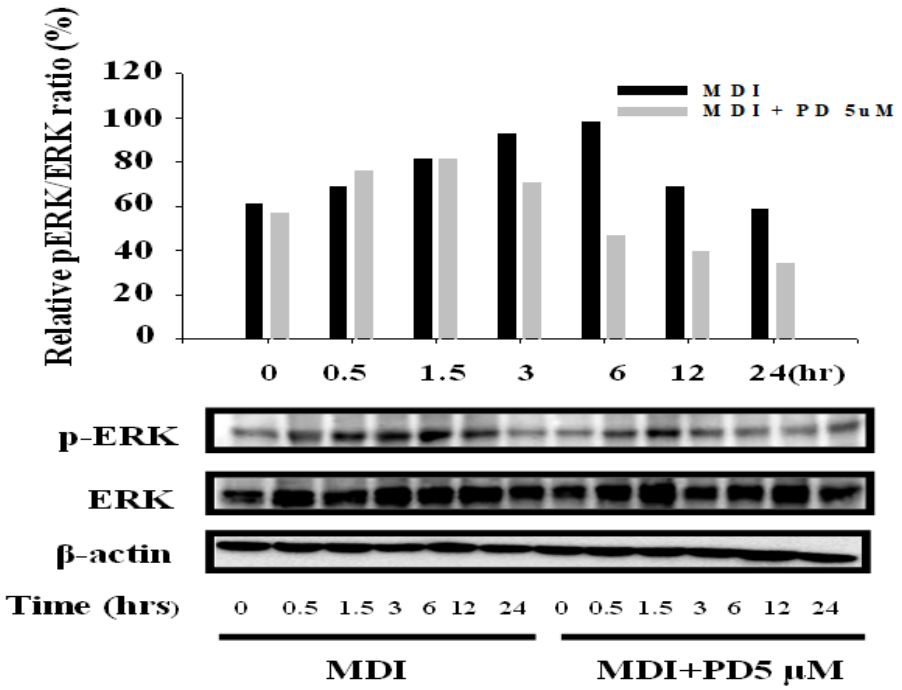

Figure 15. Effects of platycodin D on the expression of p-ERK during adipocyte differentiation.

The protein level of ERK phosphorylation in the action of PD 5 μM during 24 hr were measured by Western blot analysis adipocyte differentiation.

3.4. Effects of of PD on the expression of a p-AMPK pathway in 3T3-L1 cell

To investigate whether AMPKα activation is involved in the inhibition of adipogenesis by PD, the protein level of phosphorylated AMPKα and its substrate, phosphorylated ACC, were measured over time by Western blotting. 3T3-L1 cells exposed to the inducer were treated with 5 μM PD for 7 days during differentiation, and then adipogenesis was compared with the treatment of AICAR, a known AMPK activator **(Fig. 16)**. The results showed that the phosphorylation of AMPKα and ACC was activated by PD treatment, as well as by AICAR treatment, without changing the expression of endogenous AMPKα and ACC. However, PD-treated cells activated the phosphorylation of AMPKα at 200-fold lower concentration than AICAR. PD effectively inhibited the adipogenic transcription factors, PPARγ2 and C/EBPα, during adipocyte differentiation. These results suggest that the inhibition of adipocyte differentiation by PD is dependent on the AMPK pathway.

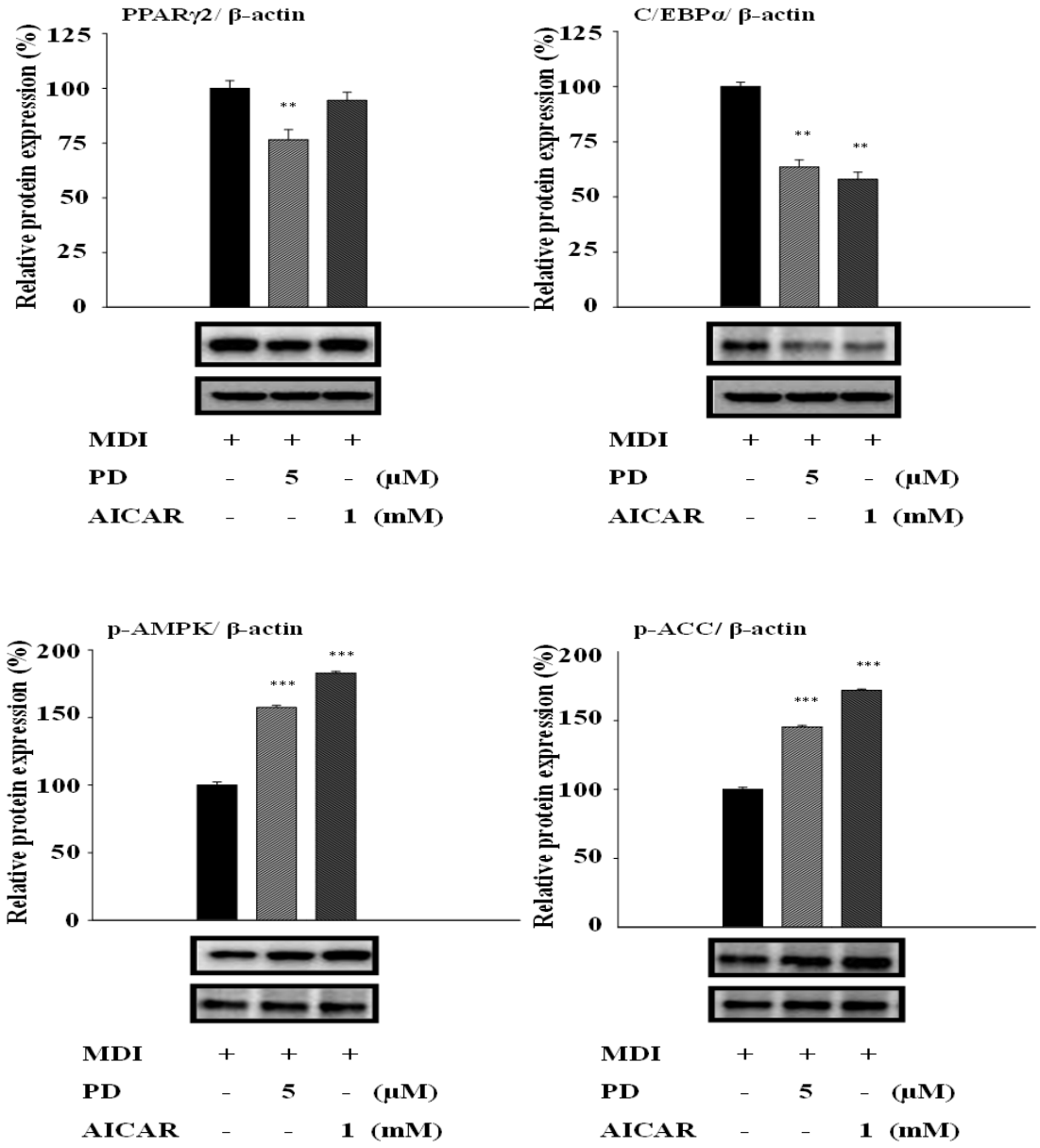

Figure 16. Effects of platycodin D on the activation of AMPKα during adipocyte differentiation.

The protein level of AMPKα and ACC phosphorylation on day 7 during adipocyte differentiation were measured by Western blot analysis and quantitated. On day 5, PPARγ2 and C/EBPα, major adipogenic transcriptional factors were detected by Western blot analysis and quantitated. The densitometry ratio of p-AMPKα and p-ACC protein expression was normalized to AMPKα and ACC. β-actin was used as a loading control. The error bars represent the standard deviations of means of three independent experiments
(**p<0.05, ***p<0.001compared to control).

3.5. Effect of platycodin D on body weight, food intake and daily energy in high fat diet mice

Based on these results, the influence of PD on obesity was investigated in C57BL/6 mice fed with a high fat diet for 8 weeks. To confirm the induction of obesity, the cholesterol level in mice serum was checked and weight gain of the high fat diet group was significantly higher than that of the normal group (HF: 32.28 ± 6.18 g; NOR: 26.57 ± 2.78 g). Eight weeks after the oral administration of 15 mg/kg of PD, the gross inspection of the high fat diet-treated PD (HP) group indicated a clear reduction in fat mass **(Fig. 17A)**.

Four weeks after the treatment, HP group showed a significant reduction in body weight compared to initial weight. However, the high fat diet-treated vehicle (HF) and high fat diet-treated AICAR (HA) group showed a steady increase in weight. At the end of the study, the body weights of the HP and HA groups were 30.70 ± 3.35 g and 44.3 ± 4.67 g, respectively. The HP and HA groups weighed less than the high fat diet group (46.66 ± 1.52 g) **(Fig. 17B)**.

A reduction in food intake was significantly observed in the PD-fed animals during the first four weeks of the administration period **(Fig. 17C, D)**. During the final fourth weeks of the study, food intake for the HP group was restored to the same level as the other groups.

A.

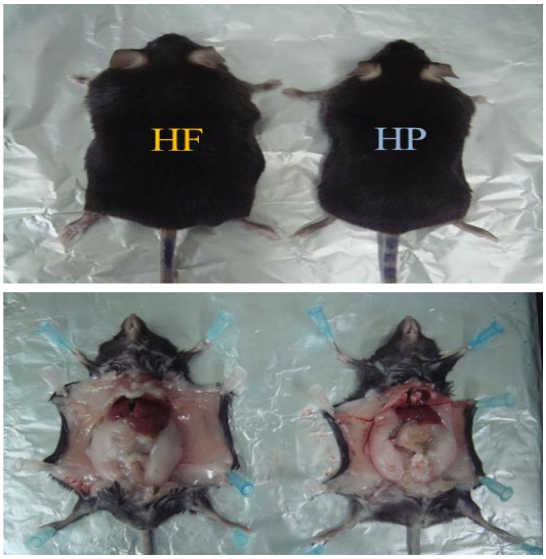

B.

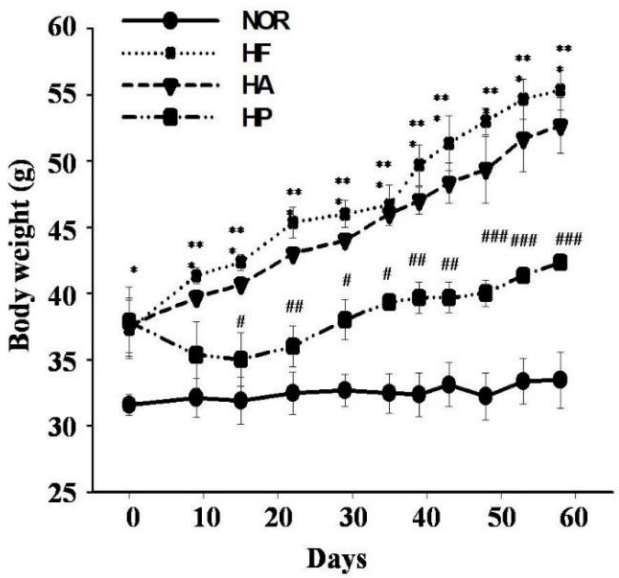

Figure 17. Effects of platycodin D on body weight gain, food intake and daily energy in C57BL/6 model-induced obesity.

The mice were divided into four groups: normal diet-treated group (NOR), high fat diet-treated group (HF), high fat diet-treated AICAR (HA), high fat diet-treated platycodin D (HP). (A) The gross inspection. (B) Body weight were recorded at 3-day intervals for 8 weeks. The error bars represent the standard deviations of means of three independent experiments (**p<0.05, ***p<0.001compared to control).

C.

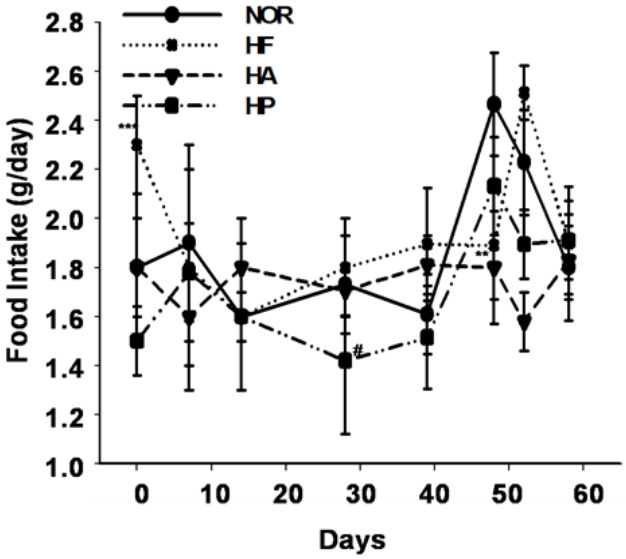

D.

Group	Initial BW (g)	Final BW (g)	Weight gain (g/day)	Food Intake (g/day)	Food Efficiency ratio
Normal	26.57 ± 0.78	28.66 ± 1.93	0.019 ± 0.012	0.258 ± 0.025	0.075 ± 0.049
HIGHFAT	32.28 ± 2.18	50.66 ± 1.52	0.305 ± 0.019	0.288 ± 0.031	1.006 ± 0.066
AICAR	32.57 ± 2.06	49.64 ± 2.65	0.261 ± 0.091	0.278 ± 0.031	0.985 ± 0.346 *
PD15	33.14 ± 2.09	35.74 ± 1.15	0.044 ± 0.033	0.254 ± 0.024	0.174 ± 0.136 **

Figure 17. Effects of platycodin D on body food intake, weight gain and daily energy in C57BL/6 model-induced obesity

The mice were divided into four groups: normal diet-treated group (NOR), high fat diet-treated group (HF), high fat diet-treated AICAR (HA) and high fat diet-treated platycodin D (HP). The error bars represent the standard deviations of means of three independent experiments (**p<0.05, ***p<0.001compared to control).

3.6. Effect of platycodin D on white adipose tissue mass and serum profiles in high fat diet mice

To investigate whether the effect of the reduction in weight by PD occurred due to a reduction in the fat size and mass of adipose tissues were examined. The size of the adipose tissue was shown by hematoxylin and eosin staining. The results showed that the HF group had increased size of adipose tissue, while the HP group had slightly decreased size of it **(Fig. 18A)**.

The micro-CT analysis demonstrated that the HP group (2693 mm^3) had a significant reduced fat mass compared to the HF group (4420 mm^3) in the abdominal region **(Fig. 18B)**. This suggested that PD decreased the epididymal adipose tissue by controlling the fat size and mass in abdominal region.

To determine whether PD improved lipid metabolism, typically plasma TG, TC, HDL-C, LDL-C and leptin were measured in serum. In this study, the serum TG in the HF group (1.34 ± 0.21 mmol/L) was higher than the NOR group (0.91 ± 0.03 mmol/L). However, the HP and HA group showed a significantly reduced serum TG of 0.86 ± 0.09 mmol/L and 0.87 ± 0.10 mmol/L, respectively. For TC, the HF group (5.24 ± 1.34 mmol/L) was still higher than the NOR (2.83 ± 0.67 mmol/L) and HP group (4.44 ± 1.45 mmol/L) was tend to be decreased in TC. In addition, the HP group significantly increased HDL-C and decreased LDL-C concentration compared to the HF group. Leptin level was highly increased in adipocyte-induced obesity, which is called leptin resistance. The HF group had a significantly higher serum leptin concentration (1.45 ± 0.17 μg/L) than the NOR group (0.75 ± 0.13 μg/L). However, the HP group (1.11 ± 0.50 μg/L) and HA group (1.13 ± 0.52 μg/L) were not higher than the HF group. There was no difference in the concentration of serum leptin between HP and HA groups **(Fig. 18C)**. These results suggest that PD improve the serum lipid profile, which might result from the decrease of lipogenesis in adipocyte differentiation.

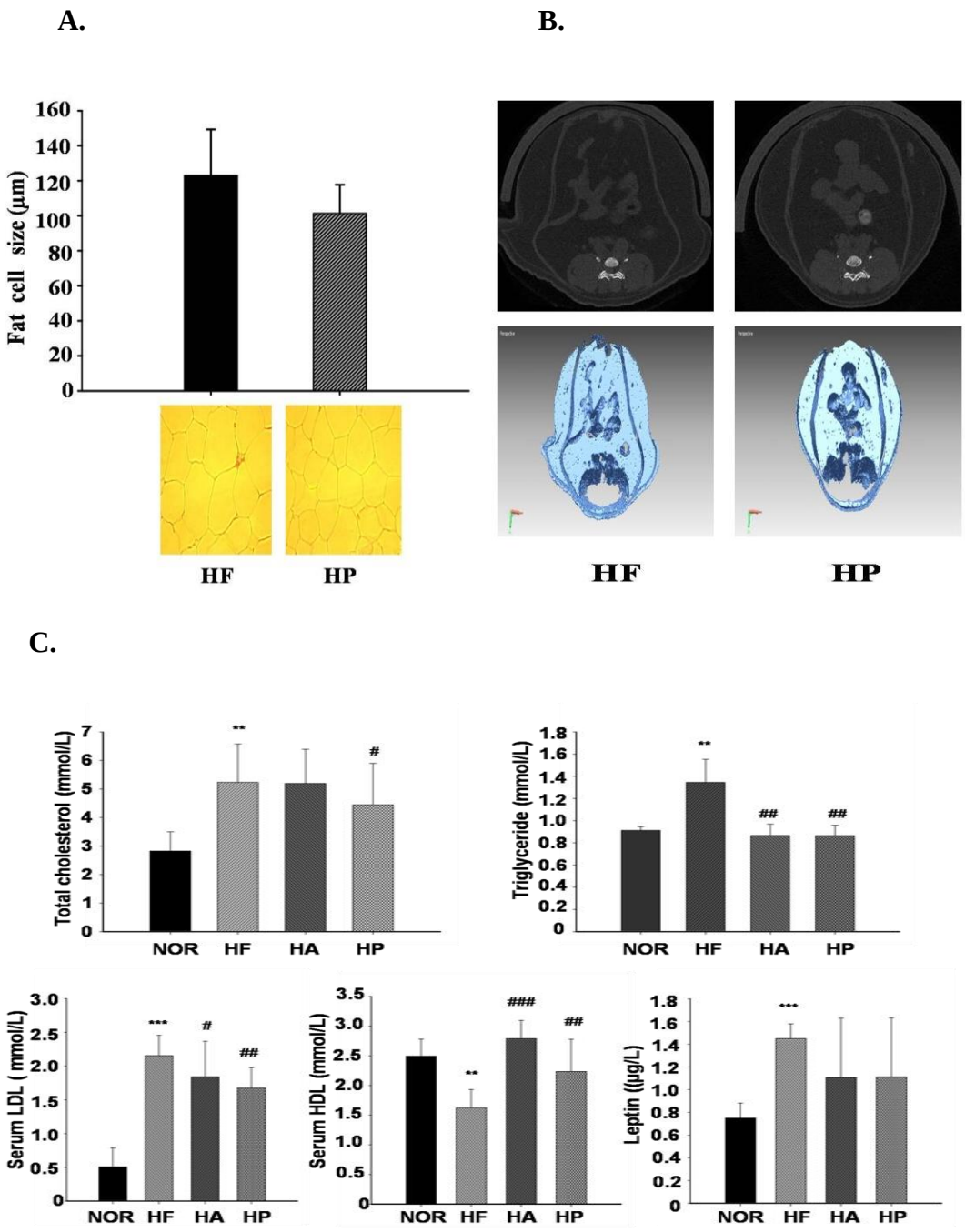

Figure 18. Effects of platycodin D on fat size, mass and serum profiles in C57BL/6 model-induced obesity.

(A) Histological analysis and quantitation of white adipose tissue size. (B) Micro-CT in abnormal region of C57BL/6 after HF and HP treatment for 8 weeks. (C) The acronyms used are as follows: total cholesterol (TC), triglyceride (TG), high density lipoprotein cholesterol (HDL-C), low density lipoprotein cholesterol (LDL-C) and leptin. Normal diet-treated group (NOR), high fat diet group (HF), high fat diet-treated AICAR (HA), high fat diet-treated platycodin D (HP).

3.7. Effects of platycodin D on the expression of proteins related to lipid metabolism in white adipose tissue

To investigate the mechanism on how PD is involved in lipid metabolism *in vivo*, Western blot analysis was done. PPARγ2, the major transcriptional factor related to adipogenesis was significantly lower in the HP and HA group than the HF group. However, the level of expression for C/EBPα was not significantly inhibited compared to PPARγ2 in the HA group. The possibility of AMPKα activation in adipose tissue was also examined. These results showed that the HP group stimulated the phosphorylation of AMPK more than the HF group in white adipose tissue. Protein expression of p-AMPKα and p-ACC of the HA group barely increased. However, the HA group did not show significantly higher protein expressions of PPARγ2 and C/EBPα than the HP group **(Fig. 19)**.

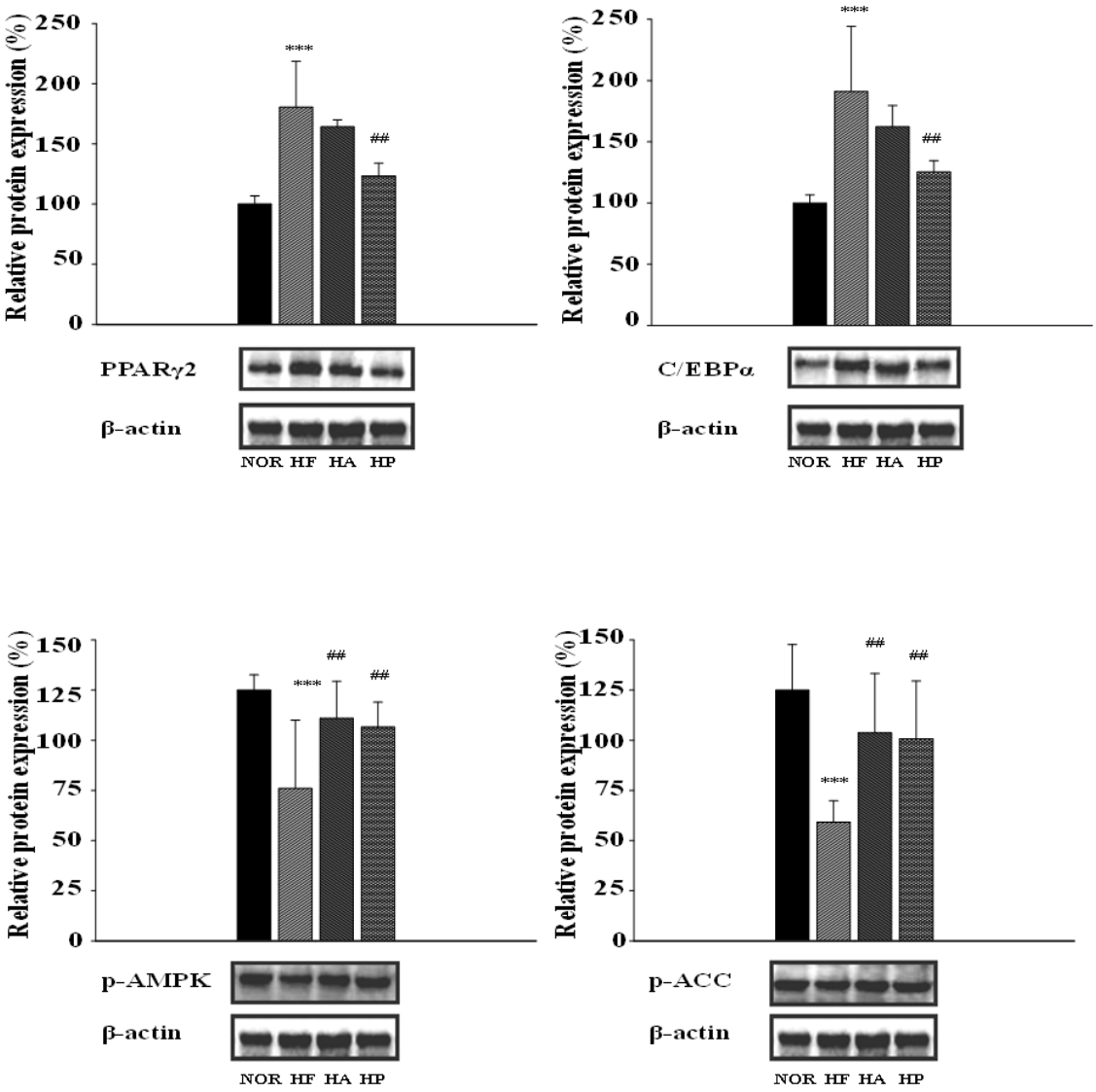

Figure 19. Effects of platycodin D on the expression of proteins related to lipid metabolism in white adipose tissue.

The expression level of PPARγ2, C/EBPα, p-AMPKα and p-ACC in white adipose tissue of C57BL/6 were measured by Western blot and quantitated. β-actin was used as a loading control. The acronyms used are as follows: normal diet-treated group (NOR), high fat diet-treated group (HF), high fat diet-treated platycodin D (HP), high fat diet-treated AICAR (HA). The error bars represent the standard deviations of means. Different superscripts indicate significant differences at $p<0.05$ according to Duncan's multiple comparison; n=3, ** $p<0.05$, *** $p<0.001$ compared to HF.

3.8. Effects of platycodin D on lipid accumulation in liver of C57BL/6 model induced obesity

Increased lipid accumulation in obesity model increase GOT, GPT value and level of triglyceride depots in the liver. We examined the effect of PD on the level of GOT and GPT, indicator of liver disease in obesity model. The level of serum GOT (58 ± 18 μM) and GPT (125 ± 18 μM) of high fat diet–treated PD group were lower than GOT (129 ± 12 μM) and GPT (307 ± 12 μM) in high fat diet group (data is not shown in this paper). Lipid accumulation of liver stained hematoxylin and eosin and the triglyceride droplets appeared round shape by space of escape. Similarly, Oil Red O staining is detected triglyceride of liver. Liver from the normal group fed tap water for 8weeks was very clearly but liver from the control group fed a high fat diet for 8weeks observed number of fatty droplet **(Fig. 20A)**. Livers from PD treated groups exhibited a decreased number of lipid droplet relative to the high fat control. To investigate mechanism of PD on fatty liver in high fat diet-fed C57BL/6 mice, we measured the level of phosphorylated AMPK that acts as a primary regulator of lipid metabolism. High fat diet feeding 8 weeks significantly decreased the level of phosphorylated AMPK in liver. Treatment of high fat fed rats with PD for 8 weeks resulted in the recovery of AMPK phosphorylation **(Fig. 20B)**. The inhibition of AMPK by lipid accumulation was associated with increased phosphorylation of SREBP-1. We next measured the level of SREBP-1, regulator of cholesterol and fatty acid metabolism has been implicated in insulin and obesity in the liver. High fat diet feeding activated SREBP-1 in the liver, while PD treatments for 8 weeks improved this effect of lipid accumulation. Our results demonstrate that high fat feeding activated SREBP-1 protein expression, which was recovered after 8 weeks of PD treatment.

A.

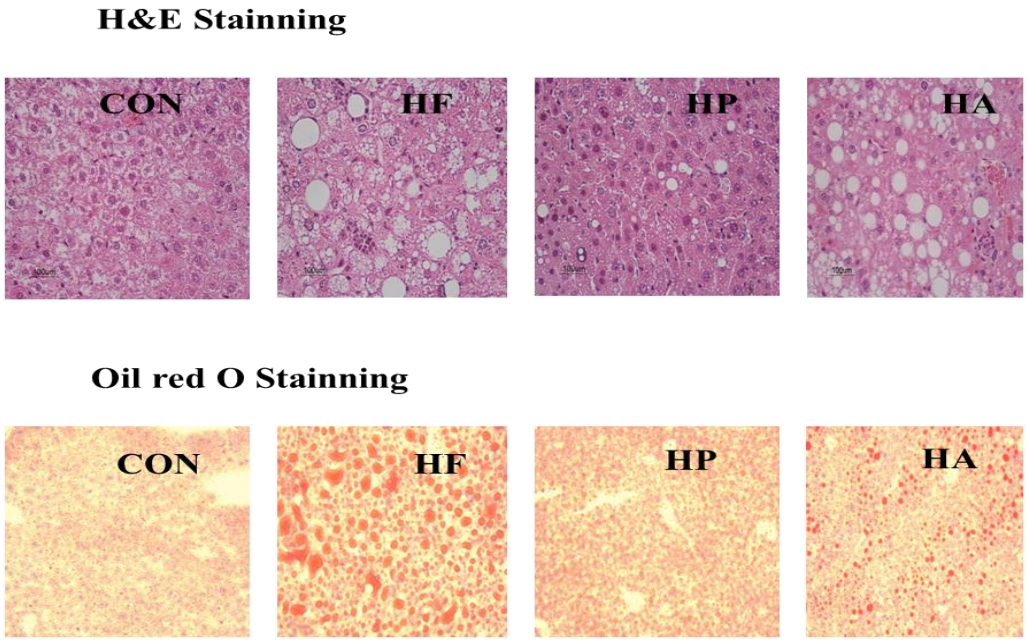

B.

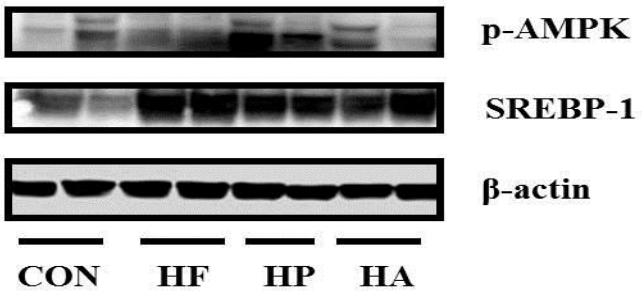

Figure 20. Effects of platycodin D on lipid accumulation in liver of C57BL/6 model induced obesity

The mice were fed normal and high fat diet (60% calories as saturated fat) for 8 weeks and it were receive oral administration of vehicle, PD 15 mg/kg for 8 weeks. At the end of the experimental period, hematoxylin and eosin and Oil Red O stained photomicrographs of liver sections are shown at ×100 (A). Also, the expression of the level of p-AMPK and SREBP-1 were measured by Western blot in the liver (B). β-actin protein was used as a loading control. Normal diet plus daily vehicle (NOR), high fat plus daily vehicle (HF), high fat plus platycodin D (HP). The error bars represent the standard deviation of the mean (n=4-5; *p <0.05, **p<0.01, *** p<0.001).

3.9. Effects of PScell on lipid accumulation inhibition activities during adipocyte differentiation

To determine the cytotoxicity of PScell, 3T3-L1 cells were treated with various concentrations of PScell (5, 7.5, 10 ㎍/㎖). The results are expressed as a percentage of the vehicle control. Treatment with 1-10 ㎍/㎖ of PScell doesn't show cytotoxicity to the 3T3-L1 preadipocyte until 8.7 ㎍/㎖. To investigate the anti-adipogenic effect of PScell on adipocyte differentiation, PScell (5, 7.5, 10 ㎍/㎖) was treated to 3T3-L1 fibroblast cells. On eight day, differentiated adipocyte were evaluated by staining with Oil Red O assay as described in the "Methods" section.

As shown in **Fig. 21** accumulated lipid contents were decreased than the lipid accumulation in control by treatment of PScell (5, 7.5, 10 ㎍/㎖) in 3T3-L1 cells. So these results showed that treatment of 3T3-L1 cells with PScells suppressed adipocyte differentiation in dose dependent manner. Among them, the one with 10 ㎍/㎖ of PScell is most effective in inhibition of lipid cell accumulation. Comparison of the results from this experiment with those with PRW, the pre-substance which exists before PScell is isolated, shows that lipid accumulation is inhibited with PRW being treated at every concentration but to a lesser extent than in those with PScell. We implemented the same experiment with PRW being treated as well as with PScell, but did not include it because the results show little difference in the extent to which PRW inhibits lipid cell accumulation compared to that with control group.

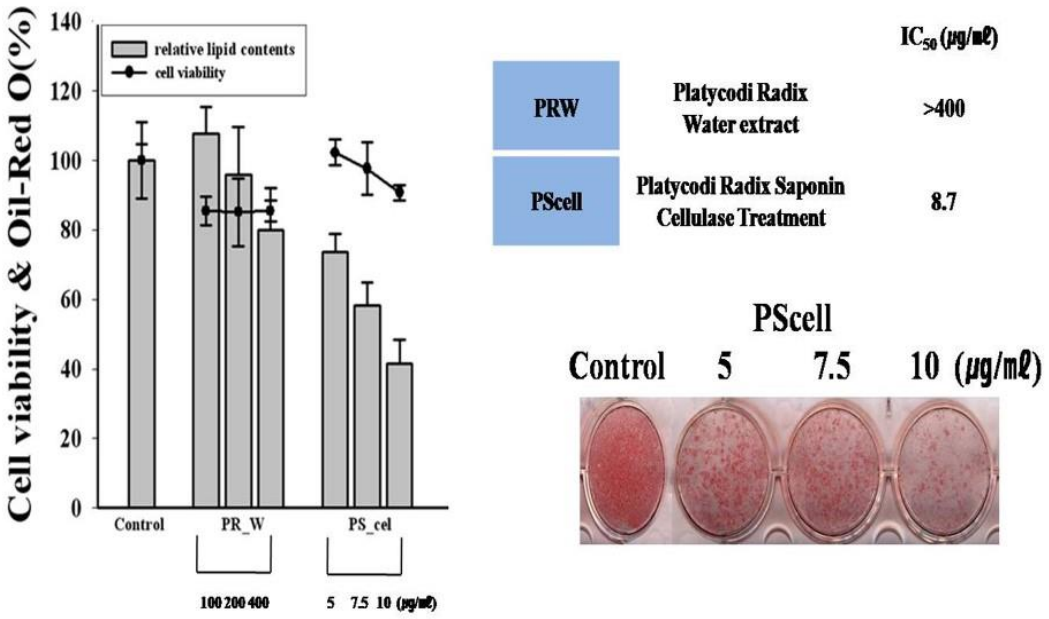

Figure 21. Effects of PScell on lipid accumulation inhibition activities during adipocyte differentiation

Cell cytotoxicity was evaluated by MTT assay. 3T3-L1 preadipocyte cells were seeded at a density of 5×10^4 per well in 96-well plates and stabilized at 37℃ for 24 hr. The cells were treated with various concentrations of sample for 48 hr in triplicate. Cells were stained with Oil Red O on day 8 after the induction of differentiation. Stained Oil Red O was eluted with 4% NP-40 in isopropanol (v/v) and the absorbance was measured at 490 nm with a spectrophotometer.

3.10. Effects of PScell on food intake and body weight gain in C57BL/6 model-induced obesity.

To investigate whether PScell could modulate obesity in animal model, male C57BL/6 mice were fed high fat diet (HFD) for 14 weeks to induce the obesity. After 6 weeks, the weight of the mice fed HFD significantly increased compared with the mice fed a standard diet ($p<0.001$). During the last 8 weeks of diet feeding, PScell was orally administered (30, 70 mg/kg/day) daily (n=8 animals per each treatment group). At the end of this experiment, the body weight of mice administrated with PScell was lower as compared with the vehicle-treated group. The results suggested that PScell has a weight-lowering effect in HFD induced obese mice. And there was no significant difference in food intake between the vehicle and HFD + PScell treated group confirming that the reduction in body weight gain in PScell administered mice was not due to reduced caloric intake in these mice model **(Fig. 22).** It should be noted that there was a significant decrease in food intake of HFD group treated with PD shown in the previous chapter, which makes the results with this experiment seem unexpected given that PScell is the PD-enriched saponin. We also implemented the same experiment with PRW 250 mg as well as with PScell, but we did not include it because the result shows almost the same degree of body weight gain in the mice administered with PRW as in high-fat group.

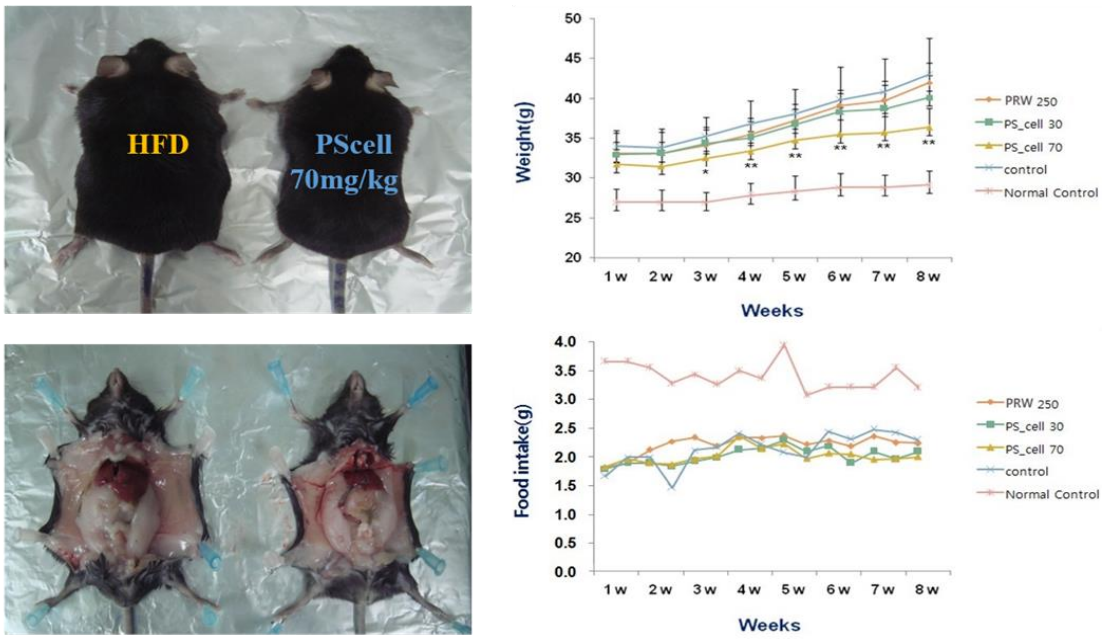

Figure 22. Effects of PScell on food intake and body weight gain in C57BL/6 model-induced obesity.

One group of C57BL/6 was fed a normal diet (Samyangsa) and others were fed with a high-fat diet containing casein 26%, maltodextrin 16%, sucrose 9%, lard 32%, soybean oil 3% and mineral mix 1% with a calorie content of 5.4 kcal/g (D-12492, Research diets) for 8 weeks (n=7). The high fat diet mice were then assigned to one of four subgroups. Group 1: The vehicle was orally administered to mice; Group 2: PRW (250 mg/kg body weight, dissolved in PBS, injection volume 6 mL/kg); Group 3: PScell (30 mg/kg body weight, dissolved in PBS, injection volume 6 mL/kg); Group 4: PScell (70 mg/kg body weight, dissolved in PBS, injection volume 6 mL/kg). Food intake were recorded once a week and body weight twice a week . The mice were sacrificed after 8 weeks for tissue and serum analysis**.**

3.11. Effects of PScell on white adipose tissue size and liver fatty droplet accumulation in C57BL/6 model-induced obesity

To examine whether the reduced body weight gain in PScell administered mice group related to decrease fat accumulation, the abdominal white adipose tissue were dissected and weighed. As shown in **Fig. 23**, the weight of adipose tissue was distinctively reduced in PScell 70 mg/kg treated group, showing that alleviated obesity in PScell treated mice is due to the reduced adiposity in the abdominal adipose tissue. Lipid accumulation of liver and abdominal adipose tissue stained hematoxylin and eosin and the triglyceride droplets appeared round shape by space of escape.

Histological analysis of abdominal adipose tissue and liver the resulted in smaller size of adipocyte and a decreased number of lipid droplet in PScell treated group compared with those in vehicle treated HFD group.

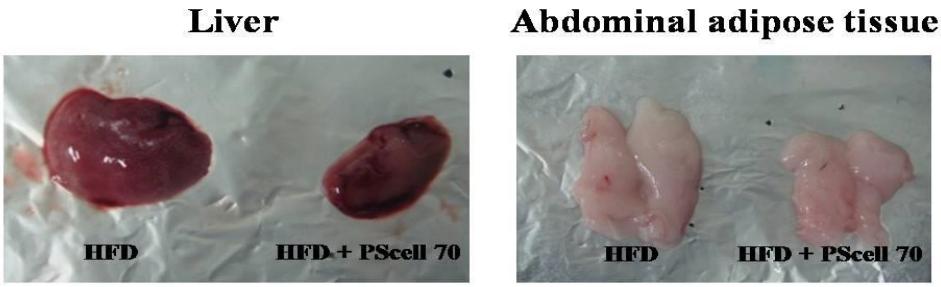

Parameter (mass)	HFD	HFD + PScell 70
Liver (mg)	399.8 ± 46.6	338.7 ± 34.9
Abdominal adipose tissue (g)	2.535 ± 0.46	2.328 ± 0.35

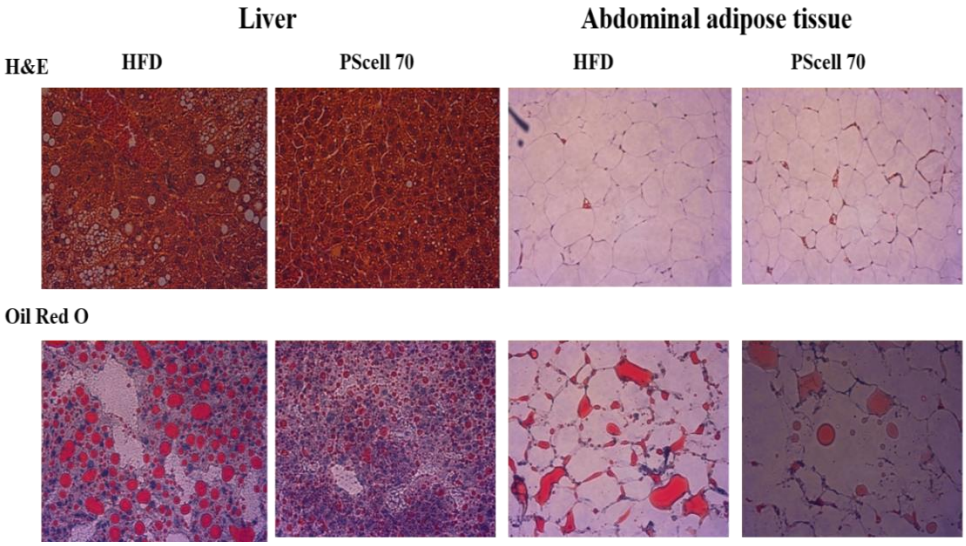

Figure 23. Effects of PScell on liver and white adipose tissue size fatty droplet accumulation in C57BL/6 model-induced obesity

The adipose tissues of mice and liver were immediately fixed in 10% formalin solution for 24 hr. These tissues were subsequently dehydrated with a series of ethanol solution, from 75% to 100%, before being embedded in paraffin wax. Cross sections were cut at 4 μm and were stained with hematoxylin and eosin. The sections were imaged by light microscopy (Olympus).

3.12. Effects of PScell on serum profiles in C57BL/6 model-induced obesity

To investigate whether alleviations in adiposity by PScell are correlated with change in serum levels of lipid metabolism makers, blood sample was collected from each group of mice. The concentration of TG, TC and fasting glucose were measured. Compare to HFD group fasting glucose serum level for HFD + PScell group were reduced by 11.4% at the end of weeks. PScell administration also significantly reduced serum total cholesterol levels for HFD + PScell groups by 12.5% and reduced serum TG levels by 11.5%. To examine the safety of PScell, the levels of PScell-induced toxicity in the liver was measured. It is not likely that elevation of serum hepatic functional makers (ALT and AST) is detected in the PScell. It is also expected that subsequent researches would achieve new findings about PScell's affect to attenuate the liver toxicity induced by HFD **(Fig. 24).**

Parameter (serum)	ND	HFD	PScell 70
ALT (U/L)	33.6 ± 1.58	69.5 ± 1.92	33.7 ± 3.52
AST (U/L)	58.3 ± 4.23	73.7 ± 6.26	68.7 ± 4.62
TG (mg/dl)	111.3 ± 5.23	136.7 ± 7.23	118.3 ± 7.74
Total Cholesterol (mg/dl)	77.7 ± 4.21	187.7 ± 12.63	150.3 ± 21.24
Glucose (mg/dl)	175.7 ± 3.86	226.3 ± 3.26	197.6± 3.85

Figure 24. Effects of PScell on serum profiles in C57BL/6 model-induced obesity

All mice were fasted for 15 hr prior to being sacrificed. Blood samples were taken from the orbit and centrifuged for the determination of biochemical parameters. The serum was stored at -70℃ until used for assays.

Ⅳ. DISCUSSION

Recently, treatments for obesity have focused on lowering fat accumulation using strategies such as appetite suppressants and digestive inhibitors [17]. However, these treatments can have serious side effects, such as weight gain, diarrhea, vomiting and increased glucose concentrations in the serum [18]. Morphological alterations in adipocytes have been found to result from the accumulation of lipid droplets and the presence of adipogenic transcription factors in the cytoplasm. The expressions of these factors in adipocytes are likely a significant cause of obesity [30] and a good strategy when treating obesity is to inhibit lipogenesis.

We observed that PD inhibited adipocyte differentiation in fully differentiated 3T3-L1 adipocytes, as revealed by Oil Red O staining and UV absorbance measurements. Furthermore, we found that PD inhibited the expression of the adipocyte-specific genes of PPARγ2 and C/EBPα, having the synergic effects of adipogenesis and lipogenesis. These results indicate that the specific targets of PD during the differentiation process of 3T3-L1 cells are PPARγ2 and C/EBPα. PPARγ2, C/EBPα are two key transcription factors of adipogenesis and lipogenesis, which are active during the early stages of adipocyte differentiation to stimulate the expression of many metabolic genes [51]. Subsequently, in the final stage of differentiation, the differentiated cells express markers characteristic of adipocyte phenotypes such as adipocyte selective fatty acid binding protein (AP2), lipoprotein lipase (LPL), acetyl-CoA carboxylase (ACC) and fatty acid binding protein (FABP) [31]. Although the mechanism by which PD inhibits adipocyte differentiation is unknown, similar results have shown that PD inhibits intracellular triglyceride accumulation by the subsequent down-regulation of PPARγ2 in 3T3-L1 cells with an IC_{50} of 7.1 μM. One of the MAPKs, ERK is reportedly involved in a mechanism that regulates the extent and duration of this activity. ERK signaling promotes adipogenesis at early stage of the process in 3T3-L1 cells and significantly detects the attenuation of activation throughout adipocyte differentiation. Initially, ERK must be activated for a proliferative stage, although later it must be shut off. Therefore, it is necessary for blocking and not for proliferation during the early stage of adipocyte differentiation. PD inhibits the adipocyte differentiation of 3T3-L1 cells through the ERK pathway after 6 hr of an MDI treatment. Some reports have

shown that a natural product treatment with the ERK pathway blocks their differentiation. Examples include quercetin [52], evodiamine [53], vitisin A [54] and resveratrol [55] in adipocytes. Fucoidan has been reported to have inhibitory effects on adipocyte differentiation via the JNK and ERK pathways [56]. Moreover, evodiamine inhibits adipogenesis through the EGFR-PKCalpha-ERK signaling pathway [53]. AMPK has been shown to be connected to p53-dependent cellular senescence, suggesting its role as an intrinsic regulator of the cell cycle in mammalian cells [57]. Phosphorylation of AMPK leads to the down-regulation of acetyl CoA carboxylase (ACC), an important enzyme for lipid biosynthesis. Phosphorylation of ACC decreases the amount of malonyl CoA, which in turn oppresses carnitine palmitoyl-CoA transferase (CPT-1), resulting an increase in fatty acid oxidation [58]. AMPK is known to be activated with AICAR, which is converted to a nucleotide that mimics the effect of AMP, and a long-term treatment with AICAR has been shown to prevent the development of diabetes in animal models [59]. A recent result shows that PD and AICAR markedly stimulate the phosphorylation of AMPK compared to the basal level. Similar results indicated that a *Platycodon grandiflorum* saponin treatment increased the phosphorylation of AMP-activated protein kinase (AMPK) in human endothelial cells [60]. Based on these results, we examined the anti-obesity effect of PD in C57BL/6 mice fed a high-fat diet for 8 weeks. A significant reduction in food intake was observed in the PD-fed animals during the first 4 weeks of the administration period. During the final four weeks of the study, food intake for the PD group was restored to the levels of the other groups. Therefore, it appears that food intake by the PD group was regulated by some factor during this time. However, it may have been that they did not eat all of their food due to the bitter taste of the PD or that another factor controlled their appetite during the first four weeks after the treatment. Similarly, the inhibition of food intake by PD was also observed in another PD-fed mouse model [42]. Leptin is an important adipose-derived cytokine that acts on receptors in the hypothalamus of the brain, regulating appetite and various aspects of metabolism [61]. Thus, it is possible that leptin affects the hypothalamus, which may have been indirectly affected by PD during the four weeks after the administration of the PD. Given that food intake returns to normal after four weeks, the inhibition of weight

gain may be attributed to AMPK activation in the insulin-AKT pathway in the animal model. A reduction in weight gain was identified by the extraction of the fat mass per unit area and by micro-CT of the abdomen region in the HP group, with significantly increased HDL-C and lowered LDL-C concentrations found compared to those in the HF group in serum. Based on these results, to confirm whether the expression of adipogenic transcription factor in adipocytes is virtually identical to that in adipose tissue, PPARγ2 and C/EBPα were examined by Western blotting. The Western blot results clearly indicate that the HP group shows decreased expression levels of PPARγ2 and C/EBPα and an increased level of AMPKα in abdominal adipose tissue in the animal model. It was also reported that AMPKα mRNA levels were decreased by the activation of PPARγ2 in the muscles and adipose tissue of high-fat-diet-induced obese mice. Similarly, it has been reported that a *platycodon grandiflorum* extract regulated FABP (free fatty acid binding protein), which is involved in free fatty acid absorption, transport, storage and that it decreased the size of the adipocytes in adipose tissue. Fatty liver is an early hallmark of non-alcoholic fatty liver disease, the most common chronic liver disease associated with insulin resistance and obesity [62]. Non-alcoholic hepatic steatosis (NASH) results from the accumulation of fat in the liver, primarily through the excessive transport of free fatty acid from visceral adipose tissue into the liver [63]. Therefore, enhanced lipogenesis in adipocytes is well known to play a major role during the development of fatty liver [64]. Increased activity levels of the serum enzymes GOT and GPT have been observed in high-fat-diet-treated mice, indicating liver toxicity. Our results show that a PD treatment significantly inhibits high-fat-diet-induced GOT and GPT activity levels. In addition, histological observations of liver tissue samples showed that lipid accumulation in the liver was significantly blocked by PD. The high-fat-diet-fed control group here showed fatty acid accumulation, as characterized by round-shaped droplets in hepatocytes. However, the group treated with PD did not show a clear droplet shape, with fewer droplets as well. Based on these results, to confirm the effects of PD on the expression levels of proteins related to lipogenesis in the liver, in this case AMPKα and SREBP-1, a Western blotting analysis was conducted. AMPK phosphorylates inactivate a number of metabolic enzymes related to lipid metabolism in order to maintain liver energy status [65].

AMPK coordinates changes in hepatic lipid metabolism. Therefore, it regulates the partitioning of fatty acids between the oxidative and biosynthetic pathways. 3-hydroxy-3-methylglutary-coenzyme A reductase (HMG-CoA reductase) and acetyl CoA carboxylase (ACC), key enzymes in cholesterol and during fatty acid synthesis were the first enzymes shown to be phosphorylated and inactivated by AMPK [66]. Our results show that PD decreased lipid accumulation of hepatocytes through the activation of AMPK and the reduction of SREBP-1, thus inhibiting the expression levels of fatty acid synthase and HMG-CoA reductase. Some reports have found that crude saponins of *platycodon grandiflorum* protect against fatty liver during chronic ethanol feeding through the activation of AMPK [67] and that a water extract of *platycodon grandiflorum* protects against hepatic steatosis in a high-fat-diet-fed C57BL/6 model [68]. Furthermore, *platycodon grandiflorum* decreases serum and liver lipid concentrations in rats with diet-induced hyperlipidemia and inhibits the process of carbon-tetra chloride-induced hepatic fibrosis [69]. Hepato-protective effects of *platycodon grandiflorum* on acetaminophen-induced liver damage in mice were also reported [70]. In conclusion, the results of the present study indicate that PD inhibits adipocyte differentiation of 3T3-L1 cells through the ERK-AMPK pathway and adiposity by PPARγ2 and C/EBPα between adipocytes and adipose tissue. The administration of PD to an animal model with high-fat-diet-induced obesity reduces fatty liver and leads to the recovery of p-AMPK. These experimental results suggest that PD is a potential candidate for treating obesity and fatty liver induced by a high-fat diet.

In addition, we attempted to investigate the fat accumulation effect of PScell, a fraction with an increased PD content, by enzymatic transformation. Based on *in vitro and in vivo* results, PScell showed a stronger inhibitory effect on lipid accumulation at a slightly lower concentration than that of PD numerically. However, it should be noted that subsequent research should include a comparison of PScell with previously commercialized compounds or PD at the protein level.

The findings here suggest that PScell is a potential candidate for treating obesity and fatty liver induced by a high-fat diet as a replacement for PD with a low yield and considering the difficulty in isolating PD in Platycodi radix.

V. REFERENCES

1. Choi YH, Yoo DS, Cha MR, Choi CW, Kim YS, Choi SU, Lee KR, Ryu SY. Antiproliferative effects of saponins from the roots of *Platycodon grandiflorum* on cultured human tumor cells. J Nat Prod 2010; 73: 1863-1867.

2. Takagi K, Lee EB. Pharmacological studies on *Platycodon grandiflorum* A. DC. Activities of crude platycodin on respiratory and circulatory systems and its other pharmacological activities. Yakugaku Zasshi 2010; 92: 969-973.

3. Lee EB. Pharmacological studies on *Platycodon grandiflorum* A. DC. A comparison of experimental pharmacological effects of crude platycodin with clinical indications of Platycodi Radix. Yakugaku Zasshi 1973; 93: 1188-1194.

4. Elijah N, Jeong JH, Lee NK, Jeong YS. Platycosides from the Roots of *Platycodon grandiflorum* and their health benefits. Prev Nutr Food Sic 2014; 19: 59-68.

5. Na YC, Ha YW, Kim YS, Kim KJ. Structural analysis of platycosides in Platycodi Radix by liquid chromatography/electrospray ionization-tandem mass spectrometry. J Chromatogr A 2008; 1189: 467-475.

6. Ishii H, Tori K, Tozyo T, Yoshimura Y. Saponins from roots of *Platycodon grandiflorum* Part 2. Isolation and structure of new triterpene glycosides. J Chem Soc Perkin Trans 2009; 1: 661-668.

7. Choi CY, Kim JY, Kim YS, Chung YC, Hahm KS, Jeong HG. Augmentation of macrophage functions by an aqueous extract isolated from *Platycodon grandiflorum*. Cancer Lett 2001; 166: 17-25.

8. Choi CY, Kim JY, Kim YS, Chung YC, Seo JK, Jeong HG. Aqueous extract isolated from *Platycodon grandiflorum* elicits the release of nitric oxide and tumor necrosis factor alpha from murine macrophages. Int Immunopharmacol 2001; 1: 1141-1151.

9. Kim YP, Lee EB, Kim SY, Li DW, Ban HS, Lim SS, Shin KH, Ohuchi K. Inhibition of prostaglandin E_2 production by platycodin D isolated from the root of *Platycodon grandiflorum*. Planta Med 2001; 67: 362-364.

10. Ha IJ, Ha YW, Kang M, Lee J, Park D, Kim YS. Enzymatic transformation of platycosides and one-step separation of platycodin D by high-speed countercurrent chromatography. J Sep Sci 2010; 33: 1916-1922.

11. Zhao HL, Harding SV, Marinangeli CP, Kim YS, Jones PJ. Hypocholesterolemic and anti-obesity effects of saponins from *Platycodon grandiflorum* in hamsters fed atherogenic diets. J Food Sci 2008; 73: 195-200.

12. Ahn KS, Hahn BS, Kwack K, Lee EB, Kim YS. Platycodin D-induced apoptosis through nuclear factor-kappa B activation in immortalized keratinocytes. Eur J Pharmacol 2006; 537: 1-11.

13. Zhao HL, Cho KH, Ha YW, Jeong TS, Lee WS, Kim YS. Cholesterol-lowering effect of platycodin D in hypercholesterolemic ICR mice. Eur J Pharmacol 2006; 537: 166-173.

14. Zhao HL, Kim YS. Determination of the kinetic properties of platycodin D for the inhibition of pancreatic lipase using a 1, 2-diglyceride-based colorimetric assay. Arch Pharm Res 2004; 27: 968-972.

15. Call EE, Kaaks R. Overweight, obesity and cancer: epidemiological evidence andproposed mechanisms. Nat Rev Canc 2004; 4: 579.

16. Van LF, Mertens IL, Block CE. Mechanisms linking obesity with cardiovascular disease. Nature 2006; 444: 875-880.

17. Fujioka K. Management of obesity as a chronic disease: nonpharmacologic, pharmacologic and surgical options. Obes Res 2002; 10: 116-123.

18. Lebovitz HE, Dole JF, Patwardhan R. Rosiglitazone monotherapy is effective in patients with type 2 diabetes. J Clin Endocrinol Metab 2001; 86: 280-288.

19. Guh DP, Zhang W, Bansback N, Amarsi Z, Birmingham CL. The incidence of co-morbidities related to obesity and overweight: a systematic review and meta analysis. Public Health 2009; 9: 122-132.

20. Spiegelman MB, Flier JS. Adipogenesis and obesity: rounding out the big picture. Cell 1996; 87: 377-389.

21. Fujioka K. Management of obesity as a chronic disease: nonpharmacologic, pharmacologic and surgical options. Obes Res 2002; 10: 116-123.

22. Gregoire FM. Adipocytes differentiation: from fibroblast to endocrine cell. Exp Bio Med 2001; 226: 997-1002.

23. Nawrocki AR, Scherer PE. The adipocyte as a drug discovery target. Drug Discov Today 2005; 10: 1219-1230.

24. Kim SH, Park HS, LeeMS, Cho YJ, Kim YS, Hwang JT. Vitisin A inhibits adipocyte differentiation through cell cycle arrest 3T3-L1 cells. Biochem Biophys Res Commun 2008; 372: 108-113.

25. Katz AJ. Mesenchymal cell culture: adipose tissue. Academic Press 2002; 77: 277-286.

26. Gregoire FM, Smas CM, Sul HS. Understanding adipocyte differentiation. Physiol Rev 1998; 78: 783-809.

27. Ross MH, Kaye GI, Pawlina W. Histology, a text and atlas. 2003.

28. Jernas M, Palming J, Sjoholm K, Jennische E, Svensson PA, Gabrielsson BG, Levin M, Sjogren A, Rudemo M, Lystig TC. Separation of human adipocytes by size: Hypertrophic fat cells display distinct gene expression. FASEB J 2006; 20: 1540-1542.

29. Skurk T, Alberti-HC, Herder C, Hauner H. Relationship between adipocyte size and adipokine expression and secretion. J Clin Endocrinol Meta 2007; 92: 1023-1033.

30. Rosen E, Eguchi J, Xu Z. Transcriptional targets in adipocyte biology. Expert Opin Ther Targets 2009; 13: 975-986.

31. Tontonoz P, Hu E, Spiegelman BM. Stimulation of adipogenesis in fibroblasts by PPARγ2, a lipid-activated transcription factor. Cell 1994; 79: 1147-1156.

32. Bost F, Aouadi M, Caron L, Binetruy B. The role of MAPKs in adipocyte differentiation and obesity. Biochimie 2005; 87: 51-56.

33. Tang QQ, Otto TC, Lane MD. Mitotic clonal expansion: a synchronous process required for adipogenesis. Proc Natl Acad Sci 2003; 100: 44-49.

34. Uto KH, Ohmori R, Kiyose C. Tocotrienol suppresses adipocyte differentiation and Akt phosphorylation in 3T3-L1 preadipocytes. J Nutr 2009; 139: 51-57.

35. Hardie DG. AMP-activated protein kinase as a drug target. Annu Rev Pharmacol Toxicol 2007; 47: 185-210.

36. Sag D, Carling D, Stout RD. Adenosine 5'-monophosphate-activated protein kinase promotes macrophage polarization to an anti-inflammatory functional phenotype. J Immunol 2008; 181: 8633-8641.

37. Yang MY, Peng CH, Chan KC. The hypolipidemic effect of *Hibiscus sabdariffa* polyphenols via inhibiting lipogenesis and promoting hepatic lipid clearance. J Agric Food Chem 2010; 58: 850-859.

38. Yang J, Maika S, Craddock L. Chronic activation of AMP-activated protein kinase-alpha in liver leads to decreased adiposity in mice. Biochem Biophys Res Commun 2008; 370: 248-253.

39. Guigas B, Bertrand L, Taleux N, Foretz M, Wiernsperger N, Vertommen D, Andreelli F, Viollet B. 5-Aminoimidazole-4-carboxamide-1-beta-D-ribofuranoside and metformin inhibit hepatic glucose phosphorylation by an AMP-activated protein kinase-independent effect on glucokinase translocation. Diabetes 2006; 55: 865-874.

40. Hawley SA, Ross FA, Chevtzoff C, Green KA, Evans A, Fogarty S, Towler MC, Brown LJ, Ogunbayo OA, Evans AM, Hardie DG. Use of cells expressing γ subunit variants to identify diverse mechanisms of AMPK activation. Cell Metab 2010; 11: 554-565.

41. Zhao HL, Sim JS, Shim SH, Ha YW, Kang SS, Kim YS. Antiobese and hypolipidemic effects of platycodin saponins in diet-induced obese rats: evidences for lipase inhibition and calorie intake restriction. Int J Obes (Lond) 2005; 29: 983-990.

42. Han LK, Xu BJ, Kimura Y, Zheng Y, Okuda H. Platycodi radix affects lipid metabolism in mice with high fat diet-induced obesity. J Nutr 2000; 130: 2760-2764.

43. Han LK, Zheng YN, Xu BJ, Okuda H, Kimura Y. Saponins from Platycodi radix ameliorate high fat diet-induced obesity in mice. J Nutr 2002; 132: 2241-2245.

44. Lee H, Kang R, Kim YS, Chung SI, Yoon Y. Platycodin D inhibits adipogenesis of 3T3-L1 cells by modulating Kruppel-like factor 2 and peroxisome proliferator-

activated receptor gamma. Phytother Res 2010; 24: 161-167.

45. Nikaido T, Koike K, Mitsunaga K, Saeki T. Two New Triterpenoid Saponins from *Platycodon grandiflorum.* Chem Pharm Bull 1999; 47: 903-904.

46. Fu WW, Shimizu N, Dou DQ, Takeda T, Fu R, Pei YH, Chen YJ. Five new triterpenoid saponins from the roots of *Platycodon grandiflorum*. Chem Pharm Bull 2006; 54: 557-560.

47. Marston A, Hostettmann K. Developments in the application of counter current chromatography to plant analysis. J Chromatogr A 2006; 1112: 181-194.

48. Loughlin WA. Biotransformations in organic synthesis. Biores Technol 2000; 74: 49-62.

49. Kratzke RA, Kramer BS. Evaluation of in vitro chemosensitivity using human lung cancer cell lines. J Cell Biochem 1996; 24: 160-164.

50. Waterborg JH, Matthews HR. The Lowry method for protein quantition. Methods Mol Biol 1994; 32: 1-4.

51. Rosen ED, Spiegelman BM. Molecular regulation of adipogenesis. Annu Rev Cell Dev Biol 2000; 16: 145-171.

52. Wang T, Wang Y, Yamashita H. Evodiamine inhibits adipogenesis via the EGFR-PKCalpha-ERK signaling pathway. FEBS Lett 2009; 583: 3655-3659.

53. Ahn J, Lee H, Kim S. The anti-obesity effect of quercetin is mediated by the AMPK and MAPK signaling pathways. Biochem Biophys Res Commun 2008; 373: 545-549.

54. Kim SH, Park HS, Lee MS. Vitisin A inhibits adipocyte differentiation through cell cycle arrest in 3T3-L1 cells. Biochem Biophys Res Commun 2008; 372: 108-113.

55. Kang L, Heng W, Yuan A. Resveratrol modulates adipokine expression and improves insulin sensitivity in adipocytes: Relative to inhibition of inflammatory responses. Biochimie 2010; 92: 789-796.

56. Kim KJ, Lee OH, Lee BY. Fucoidan, a sulfated polysaccharide, inhibits adipogenesis through the mitogen-activated protein kinase pathway in 3T3-L1 preadipocytes. Life Sci 2010; 86: 791-797.

57. Motoshima H, Goldstein BJ, Igata M, Araki E. AMPK and cell proliferation-AMPK as a therapeutic target for atherosclerosis and cancer. J Physiol 2006; 574: 63-71.

58. Hardie DG. AMP-activated protein kinase as a drug target. Annu Rev Pharmacol Toxicol 2007; 47: 185-210.

59. Song XM, Fiedler M, Galuska JW, Fernstrom M, Chibalin AV, Wallberg HH, Zierath JR. 5-Aminoimidazole-4-carboxamideribon-ucleoside treatment improves glucose homeostasis in insulin-resistant diabetic (ob/ob) mice. Diabetol 2002; 45: 56-65.

60. Kim HG, Hien TT, Han EH, Chung YC, Jeong HG. Molecular mechanism of endothelial nitric-oxide synthase activation by *Platycodon grandiflorum* root-derived saponins. Toxicol Lett 2010; 195:106-113.

61. Sweeney G. Leptin signalling. Cell Signal 2002; 14: 655-663.

62. Marchesini G, Bugianesi E, Forlani G. Nonalcoholic fatty liver, steatohepatitis and the metabolic syndrome. Hepatol 2003; 37: 917-923.

63. Varela M, Embade N, Ariz U. Non-alcoholic steatohepatitis and animal models: understanding the human disease. Int J Biochem Cell Biol 2009; 41: 969-976.

64. Jung UJ, Baek NI, Chung HG. Antilipogenic and hypolipidemic effects of ethanol extracts from two variants of Artemisia princeps pampanini in obese diabetic mice. J Med Food 2009; 12: 1238-1244.

65. Long YC, Zierath J. AMP-activated protein kinase signaling in metabolic regulation. J Clin Invest 2006; 116: 1776-1783.

66. Giri S, Rattan R, Haq E. AICAR inhibits adipocyte differentiation in 3T3L1 and restores metabolic alterations in diet-induced obesity mice model. Nutr Metab (Lond) 2006; 3:31-45.

67. Khanal T, Choi J, Hwang Y. Protective effects of saponins from the root of *Platycodon grandiflorum* against fatty liver in chronic ethanol feeding via the activation of AMP-dependent protein kinase. Food Chem Toxicol 2009; 47: 2749-2754.

68. Noh JR, Kim YH, Gang GT. Preventative effects of *Platycodon grandiflorum* treatment on hepatic steatosis in high fat diet-fed C57BL/6 mice. Biol Pharm Bull 2010; 33: 450-454.

69. Lee KJ, Choi JH, Kim HG. Protective effect of saponins derived from the roots of *Platycodon grandiflorum* against carbon tetrachloride induced hepatotoxicity in mice. Food Chem Toxicol 2008; 46: 1778-1785.

70. Lee KJ, You HJ, Park SJ. Hepatoprotective effects of *Platycodon grandiflorum* on acetaminophen-induced liver damage in mice. Cancer Lett 2001; 174: 73-81.

71. Choe SS, Huh JY, Hwang IJ, Kim JI, Kim JB. Adipose Tissue Remodeling: Its role in energy metabolism and metabolic disorders. Front Endocrinol (Lausanne) 2016; 7: 30-46.

72. Monireh D. Differential role of AMP-activated protein kinase in brown and white adipose tissure components and its consequences in metabolic diseases. J Diabetes Metab 2014; 5: 406-505.

73. Dominique L. Physiopathology of obesity and current theories on the association between an excess of fat mass and insulin resistance.ppt.

74. Philippe V, Genevieve T, Isabelle CL, Dominique L. Understanding adipose tissue development from transgenic animal models. J Lipid Res 2002; 43: 835-860.

국문요지

플라티코딘 D 와 효소에 의해 전환된 플라티코딘 D 강화분획물의 지방축적 억제효과

천연물과학 박사과정

2007-30468

이은정

길경 (*Platycodon grandiflorum* A. DC)의 유효성분이자 지표성분인 플라티코딘 D는 기존에 항암, 항산화, 항염증 등의 효능이 있는 것으로 보고가 되고 있다. 최근, 플라디코딘 D는 동물모델에서 지질대사 관련 개선능과 항비만 생리활성이 탁월한 것으로 많은 보고가 있었음에도 불구하고, 아직까지 세포수준에서 어떠한 기전으로 항비만 효과가 있는지 명확한 결과는 없고, 세포수준의 결과가 동물실험 상에서 동일하게 재현되지 않은 단점이 있다. 본 연구에서는 지방합성에 관여하는 perox-isome proliferator-activated receptor γ2 (PPARγ2)와 지방세포분화에 관여하는 mitogen activated protein kinase (MAPKs), 지방산화에 중추적 역할을 하는 AMP-activated protein kinaseα(AMPKα)의 활성을 측정하여, 지방세포에서 플라디코딘 D의 지방축척억제 효과를 확인하고 지방유도동물 모델에서 지방 억제 효과를 보고자 하였다.

플라디코딘 D가 탁월한 약리학적 가치를 가지고 있긴 하지만, 도라지 건조 중량의 미량으로 포함 되어 있고, 기존의 천연물분리 방법으로는 시간이 오래 걸리고, 수율이 낮은 단점이 있어서 플라디코딘 D를 상업적을 이용하는데 많은 어려움이 있었다. 본 실험실에서는 길경사포닌 중에 플라디코딘 D와 비슷한 화학 구조를 가진 플라디코딘 D유도체들을 효소처리를 하여 단시간 내에 플라디코딘 D로 전환, 플라디코딘 D의 함량을 높인 강화분획조성물을 만든 바 있다. 본 연구에서는 기존에 분리가 쉽지가 않던 플라디코딘 D를 대체하여 분리가 효율적이며 상업적으로 이용가능성이 있는 플라티코딘 D 강화분획물 (PScell)의 지방축척 억제효과를 확인하고자 하였다.

분화된 지방세포에 플라디코딘 D 5 μM을 처리하였을 경우 지방합성 마커인 PPARγ2와 C/EBPα가 뚜렷하게 억제되었고, 비만전사인자 (adipogenic transcription factor)인 AP2, FAS발현이 감소가 됨으로써 분화된 지방세포 내에 지방함량이 약 62.5% 정도 억제됨이 확인되었다. 또한, 지방세포 초기분화에 관여하는 것으로 알려진 유사분열 활성화 단백질 인산화효소 (MAPKkinase)는 플라디코딘 D 처리한 그룹에서 3 시간부터 24 시간까지 p-ERK를 꾸준히 억제되었다. AMPK activator로 잘 알려진 aminoimidazole carboxamide ribonucleotide (AICAR)와 비교실험에서 플라디코딘 D 5 μM투여는 AICAR 1 mM 투여보다 PPARγ2와 C/EBPα의 발현을 현저하게 억제되었고, p-AMPK와 p-ACC 발현은 유의성 있게 증가되었지만 AICAR보다는 약함이 확인되었다.

위 세포실험의 결과를 토대로, 본 실험자는 8주 동안 고지방 식이로 섭취한 C57BL/6 마우스에서 플라디코딘 D의 항비만효과를 수행하였다. 플라디코딘 D 투여그룹은 고지방식이그룹보다 경구투여 10일 이후부터 체중이 유의성 있게 감소되었고, 실험 종료 후 고지방식이그룹보다 약 16 g정도 감소된 것으로 확인되었다. 섭취량은 투여 초기 4주 동안 유의성 있게 감소되었으나 이후 4주 투여에서는 복원됨으로써 다른 그룹간 섭취량에 차이가 없었다. 플라티코딘 D 투여그룹에서 단위 면적당 지방의 부피와 지방세포 크기가 줄어들었고, 혈액내의 지질대사 개선 효과가 현저히 나타났다. 비만동물모델 지방조직에서 지방형성 (lipogenesis)의 표적 단백질인 PPARγ2와 C/EBPα의 발현정도가 억제되었고 AMPK 및 ACC의 발현이 증가되었으며, 간조직 또한 지방간의 핵심 마커인 sterol-regulatory element binding proteins 1 (SREBP-1)발현이 감소되었다.

뒤이어, 효소전환에 의해 플라디코딘 D가 강화된 분획물 (PScell)의 지방축척효과를 확인하였다. 플라티코딘 D 강화분획물을 지방세포분화 유도물질과 함께 농도별 (5, 7.5, 10 ㎍/㎖)로 처리한 결과, 분화된 지방세포에서 지방 축적이 농도별로 억제되었다. 8주간 진행된 동물실험에서 플라티코딘 D 강화분획물을 경구투여한 그룹에서는 고지방그룹보다 유의적인 체중감소와 복부지방량 감소 효과를 나타내었는데, 이것은 수치상 플라디코딘 D 와 약리활성수준이 비슷하거나 좀더 좋은 효능을 보일 것으로 예상되었다.

본 연구 결과들을 종합하여 볼 때, 플라디코딘 D와 플라디코딘 D 강화분획물은 비만 및 비만에 의해 유래된 지방간에 효과적인 약물일 것이라 기대된다. 또한, 플라디코딘 D 강화분획물은 그동안 상업화하기 어려웠던 플라디코딘 D의 대체물질이 될 수 있을 것이라 판단하지만, 산업화 과정에서는 단백질수준에서 기존 상품화 되어 있는 단일화합물이나 플라디코딘 D와 효능평가를 비교하는 후속실험이 필요할 것으로 사료된다.

주요어: 플라티코딘 D, 길경, 항비만효과, 지방억제, 지방세포, 길경사포닌,
PPAR γ 2, AMPK α, 플라티코딘 D 강화분획물

학번: 2007-30463